A Numerical Investigation of The Seismic Response of Multi-Story Frame Structures with Vertical Mass Irregularities Using Linear Time History Analysis (LTHA)

by

Ashraf Seddiki Sowrob → Reg No: 2018333558

&

Kazi Md. Adnan → Reg No: 2019333515

A thesis submitted in partial fulfillment of the requirements for the degree of Bachelor of Science in Civil Engineering.

Department of Civil Engineering
Sylhet Engineering College (SEC),
School of Applied Science and Technology,
Shahjalal University of Science & Technology (SUST),
Sylhet-3100, Bangladesh.

August, 2025

STATEMENT OF THESIS APPROVAL

The thesis entitled ‘‘**A Numerical Investigation of The Seismic Response of Multi-Story Frame Structures with Vertical Mass Irregularities Using Linear Time History Analysis**’’ by **Ashraf Seddiki Sowrob** (2018333558) and **Kazi Md. Adnan** (2019333515); Session: 2019-20, has been accepted as satisfactory in partial fulfillment of the requirement for the degree of Bachelor of Science in Civil Engineering on 12 August, 2025

Md. Assaduzzaman	Supervisor	Date approved

Assistant Professor

Department of Civil Engineering
Sylhet Engineering College (SEC)
Sylhet-3100

Dr. Mushtaq Ahmed	Co-supervisor	Date approved

Professor

Department of Civil and Environmental Engineering
Shahjalal University of Science and Technology (SUST)
Sylhet-3114

Dr. Md. Jahir Bin Alam	External	Date approved

Professor

Department of Civil and Environmental Engineering
Shahjalal University of Science and Technology (SUST)
Sylhet-3114

Sibbir Ahmed	External	Date approved

Assistant professor & Head of the dept.

Department of Civil Engineering
Sylhet Engineering College (SEC)
Sylhet-3100

DECLARATION

We now state that this undergraduate thesis work has been completed by us and has not previously been submitted somewhere else for any reason. We further attest that, to the best of our knowledge and belief, this book does not contain any previously published or written works by any other authors, with the exception of those to which appropriate citation has been made.

Supervisor
Md. Assaduzzaman
Assistant Professor,
Department of Civil Engineering,
Sylhet Engineering College (SEC)

Co - Supervisor
Dr. Mushtaq Ahmed
Professor,
Department of Civil and
Environmental Engineering,
Shahjalal University of Science and
Technology (SUST)

Ashraf Seddiki Sowrob

Registration No. 2018333558

Kazi Md. Adnan

Registration no. 2019333515

Department of Civil Engineering

Sylhet Engineering College (SEC), School of Applied Science and Technology,

Shahjalal University of Science & Technology (SUST)

Sylhet-3100, Bangladesh

ACKNOWLEDGEMENTS

Firstly, praise and appreciation to almighty Allah, for His abundant blessings during our study effort, which enabled us to complete the research successfully.

Md. Asaduzzaman, Assistant Professor, Sylhet Engineering College, our supervisor, deserve special thanks for his consistence advice, encouragement, and unwavering excitement in the completion of this thesis.

Dr. Mushtaq Ahmed, Professor, Department of Civil & Environmental Engineering, Shahjalal University of Science & Technology, is our research co-supervisor and we would like to convey our heartfelt gratitude to him for allowing us to do this research.

We wish to thank our parents for their encouragement and support. We would also want to express our gratitude to all of our friends who helped us with this research by offering advice and recommendations.

TABLE OF CONTENTS

LIST Of FIGURES

LIST OF TABLES

SYMBOLS

ε - Total strain

ε^{el} - Elastic strain

ε^{pl} - Plastic strain

σ - Effective stress

d - Damage variable (scalar, $0 \leq d \leq 1$)

D^0 - Initial elastic stiffness tensor

σ_t - Stress in tension

σ_c- Stress in compression

d_t - Damage variable in tension

d_c - Damage variable in compression

$\dot{\varepsilon pl}$ - Plastic strain rate

$\dot{\lambda}$ - Plastic multiplier

$G(\sigma)$- Plastic potential function

$\varepsilon_t{}^{pl,h}$ - Hysteretic tensile plastic strain

$\varepsilon_c{}^{pl,h}$ - Hysteretic compressive plastic strain

E_0 - Initial elastic modulus

ε_t - Total tensile strain

ε_C - Total compressive strain

$x(t)$ - Displacement vector as function of time

$\dot{x}(t)$- Velocity vector

$\ddot{x}(t)$- Acceleration vector

M - Mass matrix

C - Damping matrix

K - Stiffness matrix

$\lambda\, \ddot{x}_g(t)$- Ground excitation term

$\ddot{x_g}(t)$- Ground displacement

$\ddot{u_g}(t)$ - Ground acceleration

ξ - Damping ratio

ω -Natural circular frequency

ϕ - Mode shape matrix

$q\ (t)$ - Modal coordinate vector

I_M - Mass normalization

I_C - Damping normalization

I_K - Stiffness normalization

ξ_i - Damping ratio for mode i

ω_i - Natural frequency of mode i

$\Gamma_i \ddot{x_g}(t)$ - Modal excitation due to ground motion

ϕ_i - i-th mode shape vector

m - Mass

c - Damping coefficient

k - Stiffness

$p(t)$ - External force

x_{n+1}, x_n- Displacement at time step n+1 and n

$\dot{x_n}$, $\ddot{x_n}$ - Velocity and acceleration at time step n

β, γ - Newmark parameters

Δt - Time step size

R_n - Residual force vector

$q_i(t)$ - Modal displacement

$\dot{q_i}(t)$, $\ddot{q_i}(t)$ - Modal velocity and acceleration

p_i - Modal force

$q_{i,n}$, $\dot{q}_{i,n+1}$- Modal displacement at step n and n+1

ABSTRACT

Earthquake resistant structural design is a fundamental aspect of civil engineering, particularly for multi-story buildings where vertical mass distribution critically influences dynamic behavior. Structural vulnerability during seismic events is governed by deformation demands, force transmission mechanisms, and energy dissipation capacity. This study presents a numerical investigation into the effects of vertical mass distribution on the seismic response of reinforced concrete frame structures using Linear Time History Analysis (LTHA) conducted in the ABAQUS finite element platform. Six structural models with systematically varied mass distributions were subjected to a recorded ground motion applied in the longitudinal direction to evaluate their time dependent dynamic performance. Three primary response parameters were assessed: natural frequency, story displacement, and base shear. The analysis revealed that mass irregularity significantly affects structural response. Regular mass configurations were dominated by first mode behavior but exhibited limited damping, resulting in persistent vibrations. Irregular configurations induced complex modal interactions and non-uniform deformation, with some models showing excessive displacement that may compromise structural integrity, while others demonstrated insufficient deformation, limiting energy dissipation. Among all configurations, the model with a 50 % gradually increasing mass toward the top (Model 5) showed superior performance compared to the others. It achieved a moderate base shear response, a uniformly distributed story drift profile, and notable damping behavior, provided sufficient lateral stiffness is ensured. These characteristics indicate an effective balance between seismic force demand and deformation control, enhancing overall structural resilience. The application of LTHA was essential in accurately capturing the transient seismic behavior of mass irregular structures. The results support the adoption of configurations such as Model 5 for developing efficient, resilient, and economically feasible earthquake-resistant design strategies.

CHAPTER 1: INTRODUCTION

1.1 Background

Buildings are an important part of modern life, and keeping them safe during natural disasters like earthquakes is very important. As cities grow and more buildings are built, making sure they can handle strong ground shaking has become a big concern. Many people live and work in tall buildings, especially in busy areas where space is limited. When earthquakes happen, they can cause serious damage, which affects people's safety and daily life. That's why engineers and researchers are always looking for better ways to design buildings that stay strong and stable during earthquakes. Earthquakes are one of the most dangerous natural disasters that can seriously damage buildings and put lives at risk. As more cities grow and high-rise buildings become common in crowded urban areas, it's more important than ever to make sure these buildings are safe during strong ground shaking. Even though modern building codes have helped reduce damage, many buildings still suffer from cracks, collapses, or loss of function during earthquakes. This shows that simply following basic code rules might not always be enough to protect a building. Instead, engineers need to focus on how each building actually behaves during an earthquake, especially when the building has unusual shapes, uneven weight, or design changes. This kind of performance-based design is necessary to build structures that can stand strong and recover quickly after an earthquake.

Earthquakes are among the most devastating natural hazards, frequently causing significant economic losses, structural damage, downtime, and casualties. Past seismic events have revealed that even buildings designed according to modern seismic codes can suffer substantial damage, with a considerable portion attributed to non-structural and minor structural damage. This underscores the urgent need for a more transparent and performance-based design approach compared to traditional prescriptive codes (Lombardi & De Luca, 2020).

A key observation from these events is that structural failure often initiates at points of weakness, which commonly arise from discontinuities in a structure's mass, stiffness, or geometry (Kumar et al., 2022). This problem is exacerbated by the increasing global demand for high-rise buildings in rapidly urbanizing and densely populated areas, many of which are located in seismically active regions (Mr. S. Pol et al., 2023). Ensuring the safety and resilience of such complex urban infrastructure under seismic loads presents a significant challenge for structural engineers. Irregular building configurations, whether in plan or elevation, are consistently recognized as a major cause of failure and damage amplification during earthquakes, performing worse than their regular counterparts (Kumar et al., 2022). Seismic design codes acknowledge this by imposing restrictions on abrupt changes in mass and stiffness (Wakchaure, 2012).

Our thesis specifically targets vertical mass irregularities. This type of irregularity occurs when the seismic weight of any story is significantly greater (e.g., exceeding 150% or 200%) than that of its adjacent stories (S. Pol, 2023). Such uneven mass distribution can stem from architectural aesthetics, functional requirements, or even changes in a structure's use (e.g., adding a swimming pool on an upper floor) (KUMAR & SAMHITHA, 2024). These irregularities profoundly influence a building's dynamic behavior by altering fundamental modal parameters like natural frequencies and mode shapes, which in turn affects how the building dissipates earthquake energy. This can lead to a reduction in ductility and response modification factors, thereby increasing the probability of damage (Fanaie & Kolbadi, 2019). For instance, mass irregularity at the top or bottom of a structure can increase average peak drift demand (Katti & Balapgol, 2014). Simpler approaches like static analysis procedures are often insufficient for irregular high-rise structures because they ignore dynamic effects, nonlinearity, and the significant contribution of higher vibration modes (Lombardi & De Luca, 2020). Even RSA while a common design method, involves approximations and may not fully capture specific earthquake features or record-to-record variability without careful ground motion selection (Jain & Sharma, 2024).

Existing literature has largely focused on geometric irregularities during the initial design phase. Our research aims to fill a significant gap by investigating the impact of "unexpected irregularities," particularly those arising from uneven mass distribution due to changes in a structure's use. This is crucial for developing more comprehensive vulnerability relationships for RC structures, where irregularities emerge post-construction (Ghanem et al., 2024).

In essence, our thesis is a timely and relevant investigation into a complex problem in structural engineering, offering insights that can potentially lead to safer and more resilient building designs in earthquake-prone regions

1.2 Problem Statement of the Study

Earthquakes are among the most severe natural hazards, frequently resulting in extensive structural damage and significant loss of life. The seismic performance of a structure is primarily governed by its mass, stiffness, and damping properties. Among these, the distribution of mass particularly in the vertical direction has a critical influence on the dynamic response. Vertical mass irregularity can lead to unbalanced internal force paths, amplified inter story displacements, and localized stress concentrations, all of which can compromise structural integrity during seismic events. Moreover, such irregularities significantly modify key modal characteristics, including natural frequencies and mode shapes, thereby affecting the overall vibration behavior of the structure.

This study investigates the influence of vertical mass irregularity on seismic response using Linear Time History Analysis (LTHA) conducted in the ABAQUS finite element environment. A series of structural models with different vertical mass configurations were subjected to recorded earthquake ground motion in the longitudinal direction. The analysis focuses on evaluating key dynamic response parameters, namely story displacement and base shear, under varying mass layouts.

The primary objective is to identify mass configurations that optimize energy dissipation and reduce seismic force demands without inducing excessive deformation. By systematically assessing the effects of mass irregularity, the study provides insight into the relationship between mass distribution and structural performance during seismic loading. The results contribute to the development of performance based seismic design strategies by emphasizing the importance of vertical mass optimization in enhancing structural safety, energy dissipation capacity, and dynamic stability.

1.3 General Objectives

The main goal of this study is to carry out a detailed numerical investigation on how different vertical mass distributions affect the seismic behavior of multi-story reinforced concrete (RCC) buildings. Using the ABAQUS finite element software and the Linear Time History Analysis (LTHA) method, the research focuses on understanding how mass irregularities along the height of the structure influence its dynamic response when subjected to real earthquake ground motion. This includes examining important structural responses such as natural frequencies, story displacements, and base shear forces. The ultimate aim is to improve our knowledge of how vertical mass layout impacts the safety, stability, and performance of buildings during earthquakes, and to provide helpful recommendations for designing stronger, more resilient, and cost-effective earthquake-resistant structures in future construction practices.

1.3.1 Specific Objectives

The main objectives of this study are outlined below to guide the investigation into the seismic performance of multi-story RCC structures with varying vertical mass distributions:

a) To model and simulate a five-story reinforced concrete (RCC) structure in order to evaluate its dynamic behavior under earthquake ground motion, considering various mass irregularities along the building height.
b) To assess the structural response in terms of story displacement and base shear resulting from the applied seismic excitation across different mass distribution scenarios.
c) To identify the optimum mass irregularity configuration that achieves sufficient displacement for energy dissipation while minimizing base shear to enhance structural performance.

1.4 Organization of The Report

There are five chapters and sixteen figures in this thesis. There are also references to the publications. The following is a list of chapter-by-chapter details:

Chapter 1: Provides information about the study's background, problem statement, research objectives, limitations and scope of the study.

Chapter 2: The literature review including CDP model, dynamic equation, mathematical framework are described.

Chapter 3: Describes the methodology used for determining the material model application.

Chapter 4: The results and discussions are given.

Chapter 5: Presents conclusions, limitations of future of the study.

CHAPTER 2: LITERATURE REVIEW

2.1 Related Previous Works

Many researchers have studied how buildings react during earthquakes to find better ways to keep them safe. Over the years, different types of building weaknesses, like irregular shapes or uneven weight, have been found to cause more damage during strong ground shaking. To better understand these problems, engineers have developed different methods to study how buildings move during earthquakes. These past studies have helped improve building design and safety. However, there are still some important areas that need more attention especially when it comes to how changes in weight from floor to floor affect a building’s performance. Looking at earlier research helps us understand what has already been done and where more work is needed.

Earthquake field investigations repeatedly confirm that irregular structures suffer more damage than their regular counterparts (Wakchaure, 2012). Seismic vulnerability of cities' buildings is likely to be one of the most serious problems in earthquake regions with frequent or large-magnitude earthquakes, and particularly in fast-developing cities where the existing building stock normally includes a mixture of old and new structures. Seismic vulnerability evaluation is concerned with the structure's behavior under ground motion, damage initiation and development mechanisms, and parameters that control the potential for structural collapse or severe functional loss caused by earthquakes (S. Pol, 2023) (Ghanem et al., 2024).

The engineering community has developed various methods for seismic analysis, each with its own advantages and drawbacks, particularly concerning irregular structures: a) Linear Static Analysis: This is the simplest method, where lateral forces are approximated based on the building's fundamental period. While requiring minimal computational effort, it is limited to a single mode of vibration and is only considered appropriate for lower-height buildings with regular mass and stiffness distribution (S. Pol, 2023). b) Linear Dynamic (Response Spectrum) Analysis (RSA): RSA is a multi-mode method that estimates the maximum response of each mode using a spectrum curve, then combines these responses (Zabihullah et al., 2020). It is widely adopted as the reference design method in many codes, such as Eurocode 8 (EC8) (De Luca & Lombardi, 2017). RSA offers an improvement over static analysis by capturing higher modes. However, its approximation lies in the modal combination rule.

Given the complexities and limitations of the aforementioned methods, Linear Time-History Analysis (LTHA) presents a promising compromise. LTHA offers a time-efficient and more intuitive tool that can be easily implemented in commercial software, thus reducing computational costs and avoiding the complexities of full nonlinear modeling. It has the capability to reliably evaluate the performance of structures in serviceability conditions where behavior is essentially elastic and limited structural damage is expected. LTHA has recently been included in codes like ASCE/SEI 7-16 as an alternative to RSA within "force-based" design approaches. A critical aspect of LTHA is the selection of ground motions, often through "spectrum-compatibility," to account for specific earthquake features. This allows for a direct comparison between linear and nonlinear responses using the same ground motion suites, facilitating a better understanding of the design process and the development of simplified fragility curves. The computational efficiency of LTHA is a significant advantage; for ground motions leading to substantial nonlinear structural behavior, LTHA can be up to 40 times faster than NTHA, also inherently avoiding the convergence issues typical of nonlinear dynamic analysis. This makes LTHA a simple, intuitive, and effortless tool for practitioners (Lombardi & De Luca, 2020).

While numerous studies investigate structural irregularities (e.g., stiffness irregularity, geometric irregularity), many primarily identify the negative impact of mass irregularity (Benaied et al., 2023) (Aijaj & Rahman, 2014) (Zabihullah et al., 2020) (Fanaie & Kolbadi, 2019). Previous research extensively assesses the structural response (e.g., story displacement, base shear) resulting from existing irregularities (Kumar et al., 2022).

In conclusion, while the broader problem of seismic vulnerability and structural irregularity is well-established, and analytical tools like LTHA are gaining traction for practical applications, a clear argument can be made that there is a significant gap in the systematic investigation of optimizing vertical mass irregularity configurations within multi-story frame structures using Linear Time History Analysis.

2.2 Concrete Damage Plasticity (CDP) Model of Concrete

The Concrete Damage Plasticity (CDP) model is widely used to simulate nonlinear concrete behavior under both tensile and compressive stresses. It combines isotropic damaged elasticity with plasticity theory to capture degradation due to cracking (tension) and crushing (compression). The total strain is the sum of elastic and plastic components (Hafezolghorani et al., 2017):

$$\varepsilon = \varepsilon^{el} + \varepsilon^{pl} \tag{2.1}$$

The effective stress is computed using a degraded elastic stiffness tensor:

$$\sigma = (1-d) \cdot D^0 \cdot (\varepsilon - \varepsilon^{pl}) \tag{2.2}$$

In this context, the scalar variable d indicates damage progression from 0 (undamaged) to 1 (fully damaged), and D^0 represents the initial stiffness matrix prior to any degradation. The stress–strain relationship considering tensile and compressive behavior becomes

$$\sigma = (1-d_t)\ \sigma_t + (1-dc)\ \sigma_c \tag{2.3}$$

2.2.1 Yield Function and Flow Rule

The CDP model adopts a non-associated flow rule, where the plastic potential and yield surface do not align. Plastic flow direction is given by

$$\dot{\varepsilon pl} = \dot{\lambda} . \frac{\partial G(\sigma)}{\partial \sigma} \tag{2.4}$$

The yield function f ($\varepsilon^{pl,\,h}$, σ) defines damage initiation. In uniaxial conditions, the stress–strain relationships for tension and compression are:

$$\sigma_t = (1-d_t)\ E_0 + (\varepsilon_t - \varepsilon_t^{pl,\,h}) \tag{2.5}$$

$$\sigma_c = (1-d_c)\ E_0 + (\varepsilon_c - \varepsilon_c^{pl,\,h}) \tag{2.6}$$

2.2.2 Hardening and Damage Evolution

Plastic hardening strains $\varepsilon_c^{\text{pl, h}}$ and $\varepsilon_t^{\text{pl, h}}$ govern evolution under compression and tension. They include residual deformation due to irreversible damage:

$$\varepsilon_c^{\text{pl, h}} = \varepsilon_c - \frac{\sigma_c}{(1-\text{dc})\ E_0} \tag{2.7}$$

$$\varepsilon_t^{\text{pl, h}} = \varepsilon_t - \frac{\sigma_t}{(1-\text{dt})\ E_0} \tag{2.8}$$

The damage parameters $d_c = 1 - \frac{\sigma_c}{\sigma_{cu}}$ and $d_t = 1 - \frac{\sigma_c}{\sigma_{t0}}$ evolve with strain history, defined by stress ratios in compression and tension, respectively. These parameters allow the model to simulate cyclic degradation and softening accurately

2.3 Dynamic Equation of Motion

In linear time history analysis, the dynamic response of a multi-degree-of-freedom (MDOF) structure such as a five-story reinforced concrete frame subjected to seismic loading is governed by the fundamental equation of motion. This equation represents the equilibrium between inertia, damping, and stiffness forces in response to earthquake-induced base excitation. The general form of the equation for an MDOF system is expressed as Liang et al. (2020a):

$$M\,\ddot{x}(t) + C\,\dot{x}(t) + K\,x(t) = -\,M\,\lambda\,\ddot{x}_g(t) \tag{2.9}$$

In this equation, M, C, and K are the mass, damping, and stiffness matrices, defining inertia, energy dissipation, and restoring forces. x(t) is the displacement vector relative to the ground, with $\dot{x}(t)$ and $\ddot{x}(t)$ representing velocity and acceleration. $\ddot{x}_g(t)$ denotes the ground acceleration due to seismic excitation. λ is the influence vector, typically set as a unit vector. It indicates equal ground motion input across all degrees of freedom.

In modal analysis, the MDOF system is decoupled into independent single-degree-of-freedom (SDOF) modal equations. For each mode, the governing equation becomes:

$$\ddot{x}(t) + 2\xi\omega\,\dot{x}(t) + \omega^2\,x(t) = -\,\ddot{u}_g(t) \tag{2.10}$$

In this equation, ω denotes the natural circular frequency (rad/s), ξ is the damping ratio, $\ddot{x}(t)$ and $\dot{x}(t)$ represent the modal acceleration and velocity, and $\ddot{u}_g(t)$ refers to the ground acceleration input.

In this formulation, damping is introduced through the velocity-proportional term $2\xi\omega\, \dot{x}(t)$, where the damping ratio ξ typically ranges from 2% to 5% for reinforced concrete structures. This accounts for internal energy dissipation during vibration. The equation allows time-dependent structural responses such as displacement, velocity, and acceleration to be calculated under dynamic loading. In this study, it forms the basis for simulating structural behavior using Modal Time History Analysis in ABAQUS, particularly to evaluate the effects of mass irregularity on story displacement and base shear.

2.4 Natural Frequency Extraction in Undamped Free Vibration

Natural frequency is a fundamental dynamic property that characterizes the rate at which a structure oscillates when displaced from its equilibrium position and allowed to vibrate freely without external excitation or energy dissipation. In engineering practice, multi-story buildings and other complex structures are modeled as Multi-Degree of Freedom (MDOF) systems, where each floor or component contributes to the overall dynamic response.

The governing equation (Modal Analysis, n.d.) for free vibration in an undamped MDOF system is:

$$\mathrm{M}\,\ddot{\mathrm{x}}(\mathrm{t}) + \mathrm{K}\,\mathrm{x}(\mathrm{t}) = 0 \tag{2.11}$$

Assuming a harmonic solution of the form $x\,(t) = \phi e^{i\omega t}$, this reduces to the classical eigenvalue problem:

$$[\mathrm{K} - \lambda\,\mathrm{M}]\,\phi = 0 \tag{2.12}$$

In this context, K denotes the global stiffness matrix, M is the global mass matrix, $\lambda = \omega^2$ represents the eigenvalue, ϕ is the mode shape (eigenvector), ω is the natural circular frequency (rad/s), and $f = \omega/2\pi$ is the natural frequency in hertz.

Solving this eigenvalue problem yields multiple natural frequencies and associated mode shapes. Each eigenvalue–eigenvector pair corresponds to a specific vibration mode of the system. Accurately determining these frequencies is essential in structural design, particularly for avoiding resonance phenomena during seismic or wind-induced excitation.

2.5 Linear Time History Analysis Using Modal Superposition Method

Linear Time History Analysis (LTHA) is an essential tool for evaluating the dynamic response of structures subjected to seismic ground motions. It is based on the assumption of linear-elastic behavior, where structural properties such as stiffness and damping remain constant throughout the loading duration. The analysis is performed in the time domain and enables the detailed calculation of displacements, velocities, accelerations, and internal forces under actual or simulated ground acceleration records. For a multi-degree-of-freedom (MDOF) structural system, the equation of motion under base excitation can be expressed as:

$$M\,\ddot{x}(t) + C\,\dot{x}(t) + K\,x(t) = -\,M\,\lambda\,\ddot{x}_g(t) \tag{2.13}$$

Due to the computational complexity of solving this coupled system directly, the modal superposition method is commonly used. This technique transforms the system into a set of uncoupled equations by expressing the displacement response as a combination of the structure's natural modes (Wong, 2011):

$$x\,(t) = \phi\,q\,(t) \tag{2.14}$$

Here, ϕ is the mode shape matrix (containing eigenvectors), and q (t) represents the generalized modal coordinates. Substituting Equation (2.13) into Equation (2.14) yields (Wong, 2011):

$$M\,\phi\,\ddot{q}(t) + C\,\phi\,\dot{q}(t) + K\,\phi\,q\,(t) = -\,M\,\lambda\,\ddot{x}_g(t) \tag{2.15}$$

Pre-multiplying both sides by ϕ^T and applying the orthogonality properties of mode shapes:

$$\phi^T\,M\,\phi = I_M,\;\; \phi^T\,C\,\phi = I_C,\;\; \phi^T\,K\,\phi = I_K \tag{2.16}$$

The system reduces to a set of uncoupled second-order differential equations for each mode:

$$\ddot{q}_i(t) + 2\,\xi_i\,\omega_i\,\dot{q}_i(t) + \omega^2{}_i\,q_i\,(t) = -\,\Gamma_i\,\ddot{x}_g(t) \tag{2.17}$$

In this equation, ω is the natural frequency, ξ_i is the modal damping ratio, and $\Gamma_i = \phi^T{}_i M \lambda$ represents the modal participation factor.

The total structural response is obtained by summing the contribution of all selected modes:

$$x(t) = \sum_{i=1}^{r} \phi_i\, q_i(t) \tag{2.18}$$

Where r is the number of modes considered. In ABAQUS, this procedure is implemented through the Modal Dynamic (linear perturbation) step. The software first performs a frequency extraction to obtain eigenmodes and then uses these modes to calculate the time-dependent structural response using modal superposition. This method is computationally efficient and particularly suitable for systems where nonlinear effects are negligible, making it an appropriate approach for the present study.

2.6 Mathematical Framework of the Newmark-β Method for Linear Modal Dynamic Analysis

The dynamic behavior of linear structural systems subjected to time-dependent loads is governed by second-order differential equations. In the context of elastic systems with constant mass, stiffness, and damping properties, the equation of motion for a single-degree-of-freedom (SDOF) system is written as:

$$m\,\ddot{x}(t) + c\,\dot{x}(t) + k\,x(t) = p\,(t) \tag{2.19}$$

where x(t) is the displacement, $\dot{x}(t)$ and $\ddot{x}(t)$ are the velocity and acceleration, m denotes the mass, c is the damping coefficient, k is the stiffness, and p(t) is the external time-dependent force.

To solve this equation numerically, especially when an analytical solution is not feasible due to arbitrary loading, time integration methods are employed. Among these, the Newmark-β method is a widely accepted implicit scheme due to its balance between stability, accuracy, and ease of implementation. In this method, the time domain is discretized into equal intervals of duration Δt with t_n denoting the current time and $t_{n+1} = t_n$

+ Δt representing the next time step. The displacement and velocity at time t_{n+1} are approximated using Taylor series expansions that incorporate the unknown acceleration $\ddot{(x_{n+1})}$ and two algorithmic parameters β and γ. The Newmark method formulates the relationship based on the following expressions (Liang et al., 2020b)

$$x_{n+1} = x_n + \Delta t\, \dot{x_n} + \Delta t^2 \left(\frac{1}{2} - \beta\right) \ddot{x_n} + \beta\, \Delta t^2\, \ddot{x_{n+1}} \tag{2.20}$$

$$\dot{x_{n+1}} = \dot{x_n} + \Delta t\, \left((1-\gamma)\, \ddot{x_n} + \gamma\, \ddot{x_{n+1}}\right) \tag{2.21}$$

The parameters β and γ govern the numerical stability and damping characteristics of the method and are retained in symbolic form for generality. Substituting equations (2.20) and (2.21) into the governing equation (2.19), evaluated at t_{n+1}, yields:

$$\mathrm{m}\, \ddot{x_{n+1}} + \mathrm{c}\, \dot{x_{n+1}} + \mathrm{k}\, x_{n+1} = p_{n+1} \tag{2.22}$$

Inserting the approximated values for x_{n+1} and $\dot{x_{n+1}}$ leads to:

$$\mathrm{m}\, \ddot{x_{n+1}} + \mathrm{c}\, [\dot{x_n} + \Delta t\, (1-\gamma)\, \ddot{x_n} + \gamma\, \Delta t\, \ddot{x_{n+1}}] + \mathrm{k}\, [x_n + \Delta t \dot{x_n} + \Delta t^2 \left(\frac{1}{2} - \beta\right) \ddot{x_n} + \beta\, \Delta t^2\, \ddot{x_{n+1}}] = p_{n+1} \tag{2.23}$$

Rearranging terms and isolating $\ddot{x_{n+1}}$ yields the following expression:

$$(\mathrm{m} + \Delta t\, \gamma\, \mathrm{c} + \beta\, \Delta t^2\, k)\, \ddot{x_{n+1}} = p_{n+1} - R_n \tag{2.24}$$

where R_n represents the contribution from known quantities at time t_n , given by:

$$R_n = \mathrm{c}(\dot{x_n} + \Delta t\, (1-\gamma)\, \ddot{x_n}) + \mathrm{k}\, (x_n + \Delta t \dot{x_n} + \Delta t^2 \left(\frac{1}{2} - \beta\right) \ddot{x_n}) \tag{2.25}$$

Equation (2.23) is a scalar algebraic equation in the unknown $\ddot{x_{n+1}}$, which can be solved directly. Once the acceleration is obtained, the displacement and velocity at the next time step are updated using equations (2.20) and (2.21), respectively.

This numerical integration strategy is particularly efficient in modal dynamic analysis. In such analyses, the coupled system of equations for a multi-degree-of-freedom (MDOF) structure is first transformed into a set of uncoupled modal equations through eigenvalue decomposition:

$$\mathrm{M}\, \ddot{x(t)} + \mathrm{C}\, \dot{x(t)} + \mathrm{K}\, \mathrm{x(t)} = \mathrm{P}\, (\mathrm{t}) \tag{2.26}$$

Transforming into modal coordinates yields a series of independent equations:

$$\ddot{q_i}(t) + 2\,\xi_i\,\omega_i\,\dot{q_i}(t) + \omega^2{}_i q_i(t) = p_i(t) \tag{2.27}$$

Each of these equations is structurally identical to equation (2.19) and can be integrated independently using the same Newmark formulation.

For each mode, the response is updated as follows:

$$q_{i,n+1} = q_{i,n} + \Delta t \dot{q}_{i,n} + \Delta t^2 \left(\frac{1}{2} - \beta\right) \ddot{q}_{i,n} + \beta\,\Delta t^2\,\ddot{q}_{i,n+1} \tag{2.28}$$

$$\dot{q}_{i,n+1} = \dot{q}_{i,n} + \Delta t\,((1-\gamma)\,\ddot{q}_{i,n} + \gamma\,\ddot{q}_{i,n+1}) \tag{2.29}$$

Finally, the global displacement vector is recovered by superposing the modal contributions:

$$x(t) = \sum_{i=1}^{r} \phi_i q_i(t) \tag{2.30}$$

In summary, the Newmark-β method offers a mathematically rigorous, stable, and adaptable framework for time integration in linear dynamic systems. By keeping β and γ symbolic, the formulation remains general and applicable across a range of structural modeling scenarios, from energy-conserving to numerically dissipative schemes. This makes it especially well-suited for theoretical analysis, parametric studies, and professional finite element implementations.

2.7 ABAQUS Software

ABAQUS is a powerful finite element analysis (FEA) software developed by Dassault Systems (Khennane, 2013), widely used in engineering to simulate the behavior of structures and materials under complex loading conditions. It efficiently handles both linear and nonlinear problems in static, dynamic, thermal, and Multiphysics domains. With capabilities for modeling plasticity, viscoelasticity, damage, and large deformations, ABAQUS is especially valuable for advanced structural analysis. The standard workflow in ABAQUS includes three main stages: Preprocessing, where geometry, mesh, materials, boundary conditions, and loads are defined; Analysis, where an appropriate solver is selected (e.g., Static General, Dynamic Explicit, or Modal Frequency); and Postprocessing, where results such as stress, strain, and displacement are evaluated.

ABAQUS solves nonlinear problems using incremental-iterative methods. For time-dependent simulations like impact or seismic loading, it provides two integration schemes: implicit (ABAQUS/Standard) and explicit (ABAQUS/Explicit). In modal dynamic analysis, a frequency step extracts eigenvalues and mode shapes, which are then used in a modal dynamic step to simulate time-history responses using modal superposition. The software provides a graphical user interface (CAE) for model setup and post processing, along with Python scripting for automation and advanced customization. Furthermore, user-defined subroutines (e.g., UMAT, VUMAT) allow users to implement complex material models beyond the built-in library. Its flexibility in handling coupled physical phenomena and material nonlinearities makes it a preferred tool for simulating real-world structures.

2.8 Finite Element Model (FEM)

The Finite Element Method (FEM) is a numerical approach grounded in the principles of continuum mechanics and variational methods. It is widely used in structural dynamics to analyze complex systems that cannot be solved analytically. At the heart of FEM lies the concept of discretization, where a continuous physical domain is subdivided into smaller, finite elements connected at nodes. This process transforms an infinite-degree-of-freedom system into a manageable finite one. Two core principles govern FEM: the principle of virtual work and the principle of minimum potential energy (Khennane, 2013). The principle of virtual work ensures mechanical equilibrium by asserting that the internal and external virtual works must balance for any compatible virtual displacement. Meanwhile, the minimum potential energy principle states that a system in stable equilibrium adopts a configuration that minimizes its total potential energy.

These principles are particularly relevant in structural dynamics, where time-dependent behavior, material damping, and inertia effects must be accurately captured. By applying these foundational concepts, FEM enables the prediction of dynamic structural responses, including displacements, stresses, and natural frequencies. This makes FEM an essential tool for engineers in the design, analysis, and safety evaluation of structures under various loading scenarios.

CHAPTER 3: METHODOLOGY

3.1 Materials

In this study, the reinforcing steel used in the model is S355 grade, with a yield strength of 418 MPa. Figure 3.1 presents the stress–strain behavior of the steel, demonstrating its elastic–plastic response characteristics under loading. the concrete used had a compressive strength of 25 MPa and a corresponding tensile strength of approximately 4 MPa. Figure 3.2(a) and Figure 3.2(c) illustrate the stress–strain behavior of the concrete under compressive and tensile loading, respectively. Additionally, Figures 3.2(b) and 3.2(d) represent the damage parameters for concrete in compression and tension, where a damage value of 0 indicates an undamaged state, and a value of 1 corresponds to complete damage.

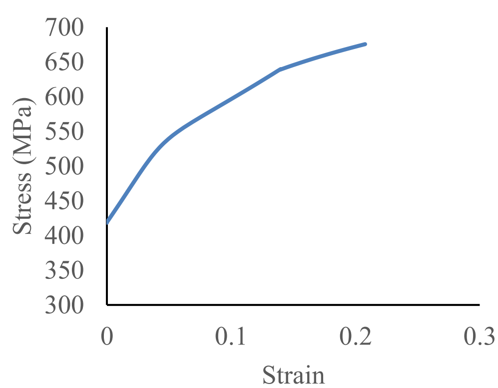

Figure 3.1: Stress – strain behaviour of steel

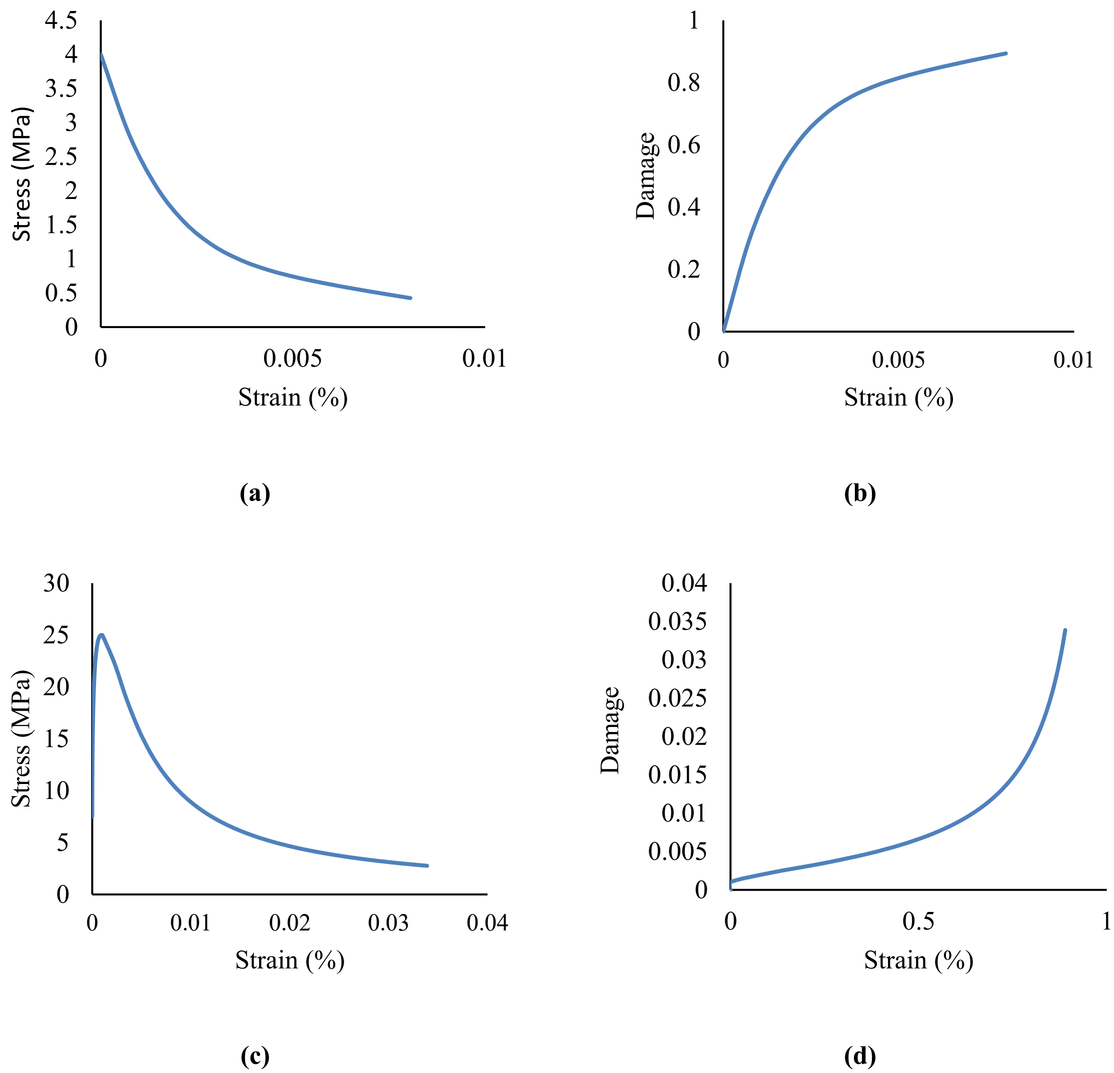

Figure 3.2: Concrete (a) Compressive stress – strain behavior, (b) Compressive damage, (c) Tensile stress – strain behavior, and (d) Tensile damage

In the numerical modeling conducted in ABAQUS, the material properties of concrete and steel were defined separately. Table 3.1 presents the key mechanical properties of each material, including modulus of elasticity, yield strength, compressive strength, density, and Poisson's ratio. These parameters are essential for accurately simulating the structural behavior under various loading conditions. Furthermore, Table 3.2 lists the plasticity parameters of concrete used in the Concrete Damage Plasticity (CDP) model.

Table 3.1: Material Properties

Parameter	Concrete (Grade 25)	Steel (S355)
Modulus of elasticity	25253 MPa	210832 MPa
Yield strength	-	418 MPa
Compressive strength	25 MPa	-
Density	2.40E-09 tonne/mm^2	7.48E-09 tonne/mm^2
Poison's ratio	0.2	0.3

Table 3.2: Plasticity Properties of Concrete

Parameter	Value
Dilation angle	30
Eccentricity	0.1
Fb0/fc0	1.16
Viscosity	0.0005
k	0.67

All material properties used in this study were obtained from the Ahmed ElKady CDP Generator for concrete (Elkady & Elkady, 2023) and the Steelmat Generator for steel (Elkady, 2023). These tools are widely recognized for generating calibrated input parameters based on previously validated experimental datasets. No experimental tests were conducted in this study; instead, the material properties were directly selected from the generators to ensure consistency with standard structural behavior. The CDP inputs represent realistic nonlinear characteristics of concrete, while the steel parameters reflect typical elastic–plastic response suitable for finite element modeling in ABAQUS.

3.2 Research Methodology

This study investigates the dynamic behavior of a multi-story reinforced concrete (RC) structure subjected to seismic loading, with a particular focus on the influence of vertical mass irregularities. The primary objective is to evaluate how varying mass distributions affect critical dynamic parameters such as base shear, natural frequency, and story displacement in order to identify an optimal configuration that enhances seismic performance. As outlined in the methodological flowchart presented in Figure 3.3, a five-story RC frame is designed in accordance with the structural design provisions of the Bangladesh National Building Code (BNBC-2020) (Gazette, 2021). The modeling is conducted in ABAQUS/CAE, involving precise geometric definition, assignment of material properties using the Ahmed ElKady CDP and Stalemate generators, component assembly, and meshing. Concrete is modeled with 8-node solid elements (C3D8R), while reinforcing steel is represented by 2-node truss elements (T3D2). Interaction techniques such as embedded constraints, tie connections, and surface-based coupling are applied to ensure realistic force transfer and structural behavior.

The simulation process comprises two key analysis steps: (1) a frequency step for eigenvalue and mode shape extraction, and (2) a linear modal dynamic step using time-history input. Six distinct vertical mass configurations are applied across the story levels to simulate mass irregularities. A longitudinal earthquake ground motion record is used to excite the structure and generate dynamic response data.

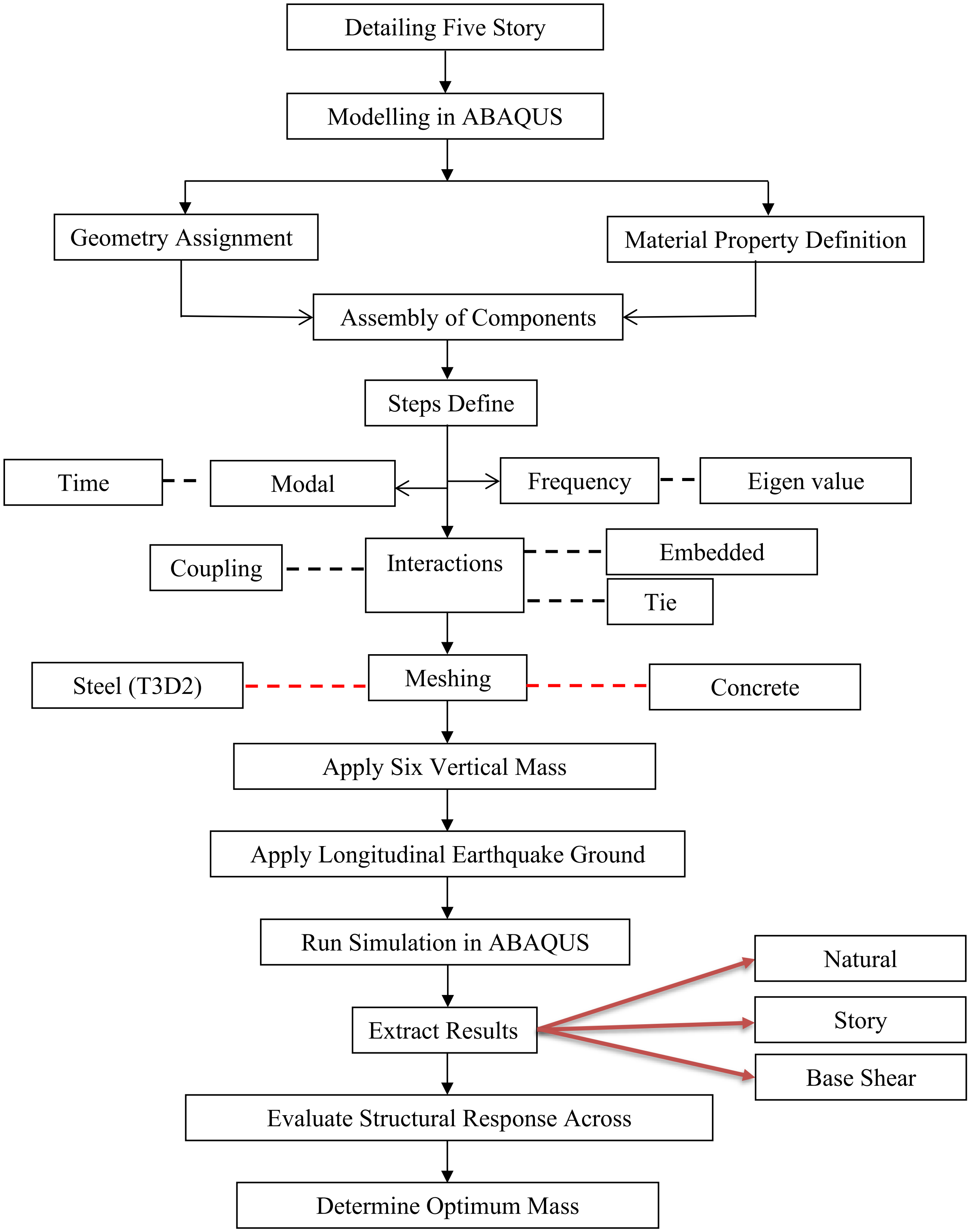

Figure 3.3: Flowchart of the methodology

A comparative analysis is performed on the simulation outputs. Key response metrics - such as base shear, inter-story displacement, and natural frequencies are extracted and evaluated across configurations. The results highlight the significant role of mass distribution in affecting stiffness, damping characteristics, and seismic amplification, offering valuable insights for performance-based seismic design of irregular RC buildings.

3.3 Detailing of The Frame Structure

In this study, a five-story serviceable frame structure was designed and detailed specifically for the Sylhet seismic zone in accordance with the guidelines set by the Bangladesh National Building Code (BNBC 2020). The adopted structural system is a moment-resisting frame, developed to support both vertical and lateral seismic loads. Figure 3.4(a) illustrates the elevation view of the frame, where each story has a uniform height of 3 meters, and seismic ground motion is applied horizontally at the base to simulate earthquake excitation. Figure 3.4(b) presents the plan view, which consists of a single bay in each direction with a span of 5 meters, forming a square layout. The frame includes four corner columns, each with a cross-section of 300 mm × 300 mm, and beams sized 250 mm × 380 mm are provided between columns in both directions.

Figure 3.4(c) shows the typical column reinforcement details. Each column contains a total of eight longitudinal bars, comprising four 20 mm diameter bars at the corners and four 16 mm diameter bars placed between them. Lateral ties of 10 mm diameter are provided at 100 mm spacing throughout the height of the column. All columns extend continuously from the foundation to the top story to ensure vertical load transfer and moment continuity. Figure 3.4(d) details the beam reinforcement layout. Each beam contains three 16 mm diameter longitudinal bars at the top and two 16 mm diameter bars at the bottom, ensuring flexural capacity under seismic loading. 10 mm diameter stirrups are provided at 150 mm spacing to resist shear forces. A 25 mm clear cover is maintained from the outer faces of the beam and column to the reinforcement on all sides to ensure adequate protection against corrosion and fire.

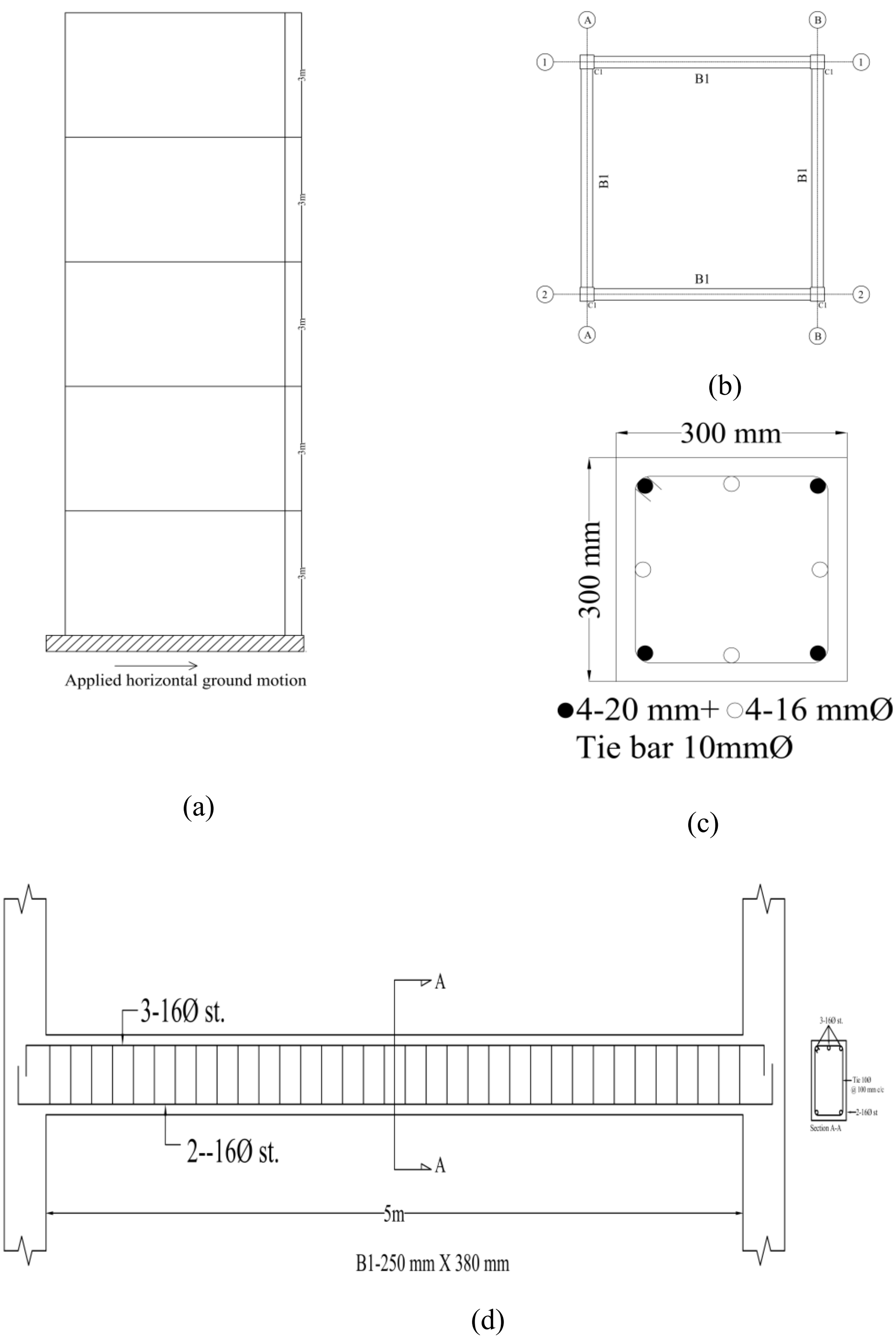

Figure 3.4: Detailing of the frame (a) Elevation, (b) Plan, (c) Typical column, and (d) Typical Beam

3.4 Mass Distribution Configuration

This study conducted a numerical investigation using ABAQUS to evaluate the influence of vertical mass distribution on the seismic response of multi-story frame structures subjected to horizontal earthquake ground motion. As outlined in Table 3.3, six structural models were developed with distinct mass configurations applied across five stories to assess their dynamic behavior.

Table 3.3: Mass Distribution

Model	**Mass (kg) along the story**					**Mass pattern**
	1st	**2nd**	**3rd**	**4th**	**5th**	
Model - 1	0	0	0	0	0	No Mass
Model - 2	3000	3000	3000	3000	3000	Uniform
Model - 3	3000	3750	4688	5860	7325	25 % Gradually increasing
Model - 4	7325	5860	4688	3750	3000	25 % Gradually decreasing
Model - 5	3000	4500	6750	10125	15188	50 % Gradually increasing
Model - 6	15188	10125	6750	4500	3000	50 % Gradually decreasing

Model 1 acted as the reference case, with no mass assigned along the story height, used to observe the baseline response of the frame. Model 2 applied a uniform mass of 3000 kg per story, which corresponds to approximately 1.2 KN/m^2 of dead load—a standard base value recommended by the Bangladesh National Building Code (BNBC 2020) for floor systems. Models 3 and 4 incorporated 25% gradually increasing and decreasing mass distributions, respectively, where Model 3 was top-heavy and Model 4 bottom-heavy. Models 5 and 6 followed 50% gradually increasing and decreasing mass profiles, introducing more significant vertical mass irregularity.

These configurations enabled a comparative evaluation of key structural responses—including natural frequency, story displacement, base shear, and inter-story drift—under identical ground excitation. The objective was to identify an optimum mass distribution that improves seismic performance while maintaining practical feasibility in structural design.

3.5 Ground Motion Selection and Application

In this study, horizontal ground motion was applied to evaluate the seismic performance of multi-story frame structures. Due to the unavailability of recorded strong-motion data for the Sylhet seismic zone, a representative ground motion from the India–Bangladesh Border earthquake, which occurred on February 6, 1988, was adopted. The corresponding acceleration time-history, which illustrates the variation of ground acceleration over time, is shown in Figure 3.5. This motion was recorded at Dauki station, India, and obtained from the Department of Earthquake Engineering, Indian Institute of Technology (IIT), Roorkee.

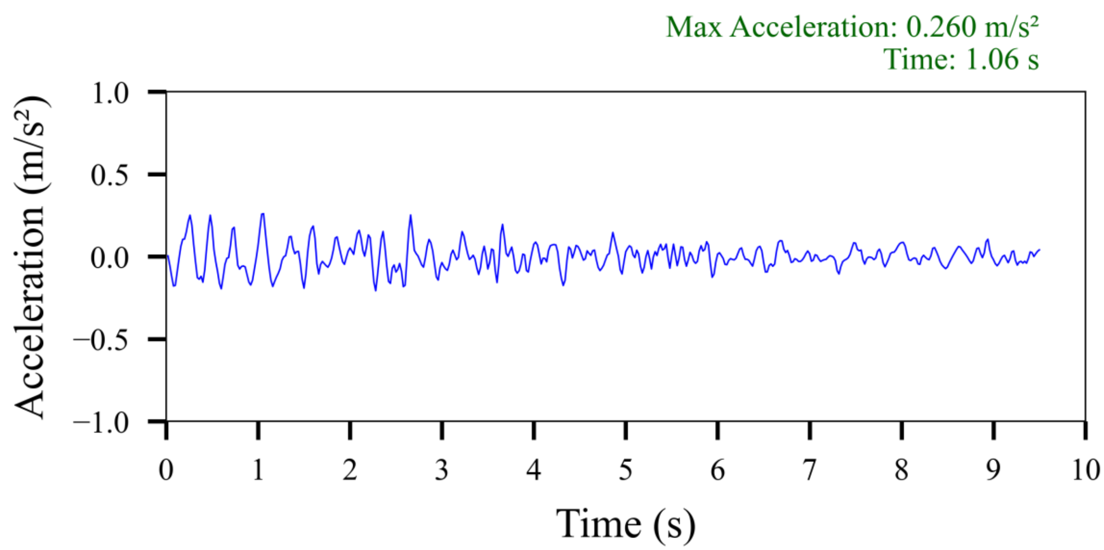

Figure 3.5: Applied Ground Motion (India - Bangladesh Border, 1988)

The selected ground motion was chosen for its tectonic similarity and geographical proximity to the Sylhet fault system. The longitudinal component of acceleration was applied as seismic input in the analysis. The associated ground motion parameters, such as recording location, site geology, and peak ground acceleration, are summarized in Table 3.4.

Table 3.4: Ground Motion Data

Parameter	Value
Region	India
Station	Dauki
Latitude	24.6880
Longitude	91.5700
Depth	15.0 km
Magnitude	5.8
Site geology	Soil
Hypo central distance	80.5 km
PGA	0.260 m/s/s
Direction	Longitudinal

By applying this recorded excitation in the horizontal direction, the study achieves a realistic simulation of lateral earthquake forces. This enables accurate evaluation of key dynamic responses, including story displacement, base shear, and inter-story drift, thereby contributing to a more comprehensive understanding of the seismic behavior of frame structures.

3.6 Essential Response Indicators in Linear Time History Analysis

In seismic performance evaluation using Linear Time History Analysis (LTHA), it is essential to understand how a structure behaves under real earthquake ground motion. This is achieved by analyzing specific response parameters that reflect the dynamic interaction between structural mass, stiffness, and damping. Among these, displacement, base shear, and frequency are considered the most fundamental and informative. Displacement provides insight into the relative movement, deformation demand, and serviceability of structural components. Base shear represents the total lateral force transmitted to the foundation, serving as a key indicator of internal force demand and lateral load resistance. Frequency defines the natural vibration characteristics of the structure, helping to assess modal participation and potential resonance under seismic excitation. Together, these three parameters offer a comprehensive understanding of both the strength and dynamic response of a structure, forming a solid foundation for assessing safety, stability, energy dissipation, and overall design performance during earthquake events.

3.6.1 Frequency

Frequency is a dynamic property that characterizes how rapidly a structure vibrates when subjected to external excitation, such as earthquake ground motion. It is determined through modal analysis by solving the eigenvalue problem, and each natural frequency corresponds to a unique deformation mode of the structure. Lower natural frequencies are associated with flexible systems that undergo larger movements but potentially absorb more energy, whereas higher frequencies indicate stiffer systems that respond more rapidly but can experience greater accelerations. The distribution of natural frequencies across multiple modes provides insight into how the structure participates in vibrational energy at various scales, and whether it is prone to resonance, where the frequency of ground motion matches the natural frequency of the building, resulting in amplified responses. In structures with irregular mass distribution, the variation in natural frequencies can cause complex modal interactions and significantly affect the time history response. Understanding frequency behavior is thus essential for predicting how the structure will perform under seismic loading and for developing design strategies that avoid resonance and excessive dynamic amplification.

3.6.2 Story Displacement

Displacement is one of the most fundamental response parameters in seismic analysis, representing the relative movement of different levels of a structure during ground motion. In the context of time-dependent earthquake loading, displacement allows engineers to assess the degree to which structural components deform under seismic forces. It is particularly important for evaluating inter story drift, which is the difference in displacement between consecutive floors and a key indicator of both structural and non-structural damage potential. Excessive displacement may compromise the serviceability and stability of a structure, even if it remains standing. It can lead to functional loss, damage to partition walls, glazing, and other non-structural elements, and in severe cases, progressive structural failure. In multi-story buildings with vertical mass irregularities, displacement responses vary significantly across floors, and understanding this behavior is crucial for identifying weak zones, assessing energy dissipation, and ensuring compliance with seismic design criteria.

3.6.3 Base shear

Base shear refers to the total lateral force transmitted from the superstructure to the foundation over the course of seismic excitation. It reflects the cumulative inertial force developed as the mass of the structure accelerates during an earthquake. In engineering practice, base shear is a critical parameter for evaluating the overall lateral force demand on the structural system. It directly influences the design and sizing of key lateral load resisting elements such as shear walls, braced frames, and moment resisting frames. Higher base shear values typically occur in structures with significant mass or stiffness at lower levels, while more flexible structures may show moderate base shear but larger displacements. Monitoring base shear helps ensure the foundation system and lower stories are adequately designed to resist the seismic forces without failure. It also provides insight into how mass distribution affects force transmission mechanisms, especially when comparing different structural configurations.

3.7 Mass Distribution Effects on Modal Behavior

Modal analysis is a fundamental technique in structural dynamics used to determine a system’s natural frequencies and corresponding mode shapes by solving the eigenvalue problem. Each mode represents a distinct vibrational deformation pattern in which the structure oscillates freely without external excitation. In this study, fifteen modes were extracted for each of the six structural configurations to capture their complete dynamic characteristics under longitudinal seismic loading.

As presented in Figure 3.7, the mode shape framework for the model with 50 % gradually increasing mass distribution (Model 5) illustrates the displacement profile associated with each vibration mode. These mode shapes describe how deformation develops spatially across the structure for increasing modal frequencies. A damping ratio of 5 % was applied exclusively to the first mode to realistically simulate energy loss associated with fundamental lateral sway. Damping was intentionally excluded from higher modes, as it introduced excessive numerical attenuation and led to unrealistic dynamic responses beyond the fundamental range.

The modal frequency values for this top-heavy configuration range from 1.26 cycles/time in the first mode to 13.13 cycles/time in the fifteenth mode. A gradual increase in frequency with mode number indicates a stiffer dynamic response in higher-order modes and reflects typical behavior for multi-degree-of-freedom structures.

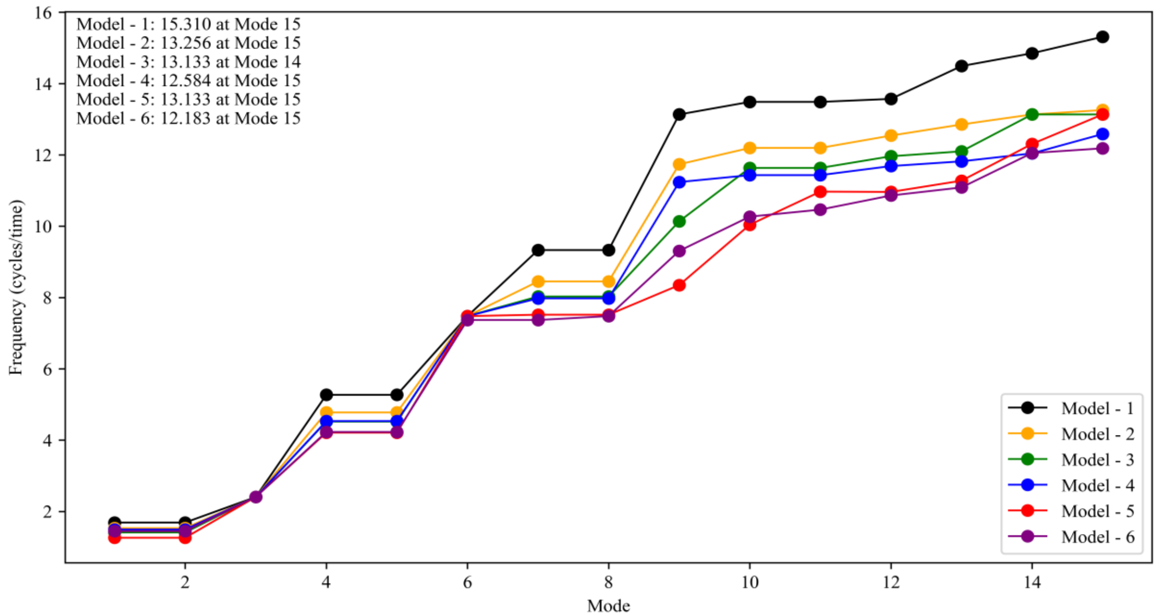

Figure 3.6: Frequency distribution of different models

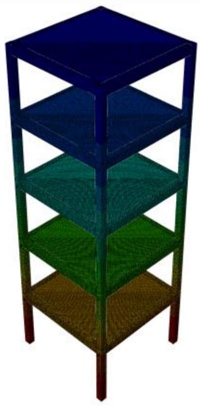 Mode: 1 Frequency: 1.26 cycles/time	 Mode: 2 Frequency: 1.26 cycles/time	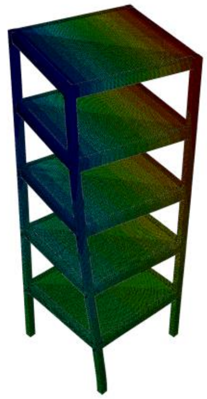 Mode: 3 Frequency: 2.40 cycles/time	 Mode: 4 Frequency: 4.22 cycles/time	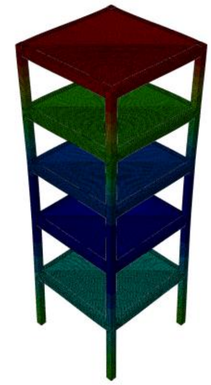 Mode: 5 Frequency: 4.22 cycles/time
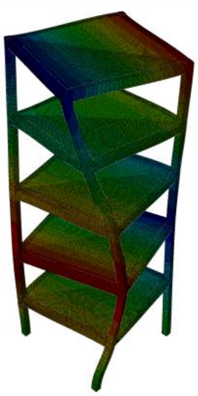 Mode: 6 Frequency: 7.48 cycles/time	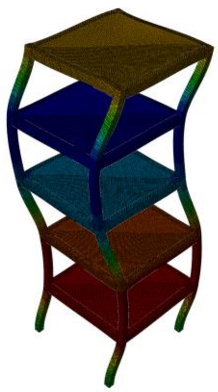 Mode: 7 Frequency: 7.52 cycles/time	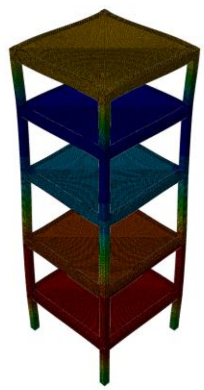 Mode: 8 Frequency: 7.52 cycles/time	 Mode: 9 Frequency: 8.34 cycles/time	 Mode: 10 Frequency: 10.04 cycles/time
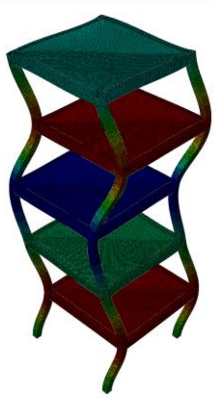 Mode: 11 Frequency: 10.97 cycles/time	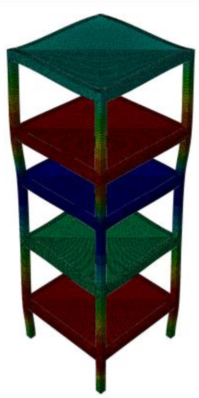 Mode: 12 Frequency: 10.97 cycles/time	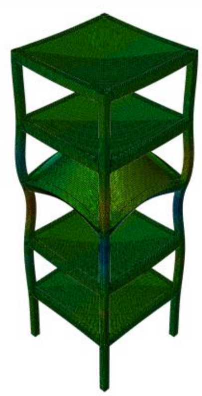 Mode: 13 Frequency: 11.27 cycles/time	 Mode: 14 Frequency: 12.31 cycles/time	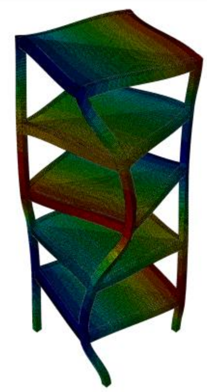 Mode: 15 Frequency: 13.13 cycles/time

Figure 3.7: Mode framework for Model - 5

Figure 3.6 illustrates the frequency distribution across all six models and offers critical insight into how mass distribution influences structural stiffness. The first mode in each case represents the lowest frequency and captures the dominant global sway. The structure without additional mass (Model 1) reaches the highest natural frequency, 15.310 cycles/time at the fifteenth mode, indicating the greatest stiffness among all configurations. On the opposite end, the system with 50 % gradually decreasing mass (Model 6) exhibits the lowest peak frequency of 12.183 cycles/time, reflecting increased flexibility due to heavier base mass. The model with 50 % gradually increasing mass (Model 5) shows a moderate maximum frequency of 13.13 cycles/time, suggesting a balance between top-heavy mass distribution and intermediate stiffness.

The frequency curves of all models show a point of convergence near the sixth mode, indicating a transition region where structural dynamic behavior becomes increasingly localized. This convergence reflects similarities in stiffness across models for specific deformation patterns. In general, higher natural frequencies imply stiffer responses and shorter vibration periods, while lower frequencies indicate more flexible behavior and longer periods. Understanding this distribution is essential for predicting how each model will respond under seismic excitation and for evaluating modal contributions to structural displacement and force demand.

3.8 Displacement Response Evaluation Across Structural Models

To evaluate the time-dependent deformation behavior of the structural models, story-level displacement responses were analyzed under seismic excitation using Linear Time History Analysis. Displacement is a key response parameter that reflects how structural motion propagates vertically across the building height and indicates the degree of inter story drift and overall flexibility. By observing the variation in displacement amplitude and timing across different floors, valuable insights can be drawn regarding the effect of mass distribution on structural dynamics. This section presents a comparative assessment of the displacement–time history plots for all six mass configuration models, allowing for the identification of deformation patterns, energy dissipation characteristics, and relative stiffness along the building height.

3.8.1 Dynamic Displacement Response of Model - 1

Figure 3.8 illustrates the displacement time response of each story in Model 1, a structural configuration without any additional mass along the height. The graph shows that displacement amplitudes gradually increase from the base to the upper levels, with the fifth story reaching the maximum value of 58.386 mm at 3.44 seconds. In contrast, the lower stores, such as the first and second, experience their peak displacements earlier, around 2.52 seconds. This timing difference across levels indicates that the dynamic effect introduced at the base does not impact all floors simultaneously; instead, the response develops upward, with upper stories reacting slightly after the lower ones. Such a delay reflects the natural progression of structural movement as force propagates through the building. The displacement curves at the lower stores also show more closely spaced oscillations, suggesting that higher frequency components contribute more prominently at these levels. In contrast, the upper stories exhibit broader waveforms, indicating longer-period motion with greater amplitude. This variation implies that the response characteristics vary with height, with more complex motion concentrated near the base and smoother displacement patterns appearing toward the top. Overall, the displacement curves across all stores remain smooth and consistent, without sudden changes or irregularities. This indicates that the structure responds as a unified system, with its motion primarily influenced by geometry, stiffness, and support conditions. The absence of added or uneven mass ensures a balanced response, making the dynamic characteristics of the structure easier to observe under external loading.

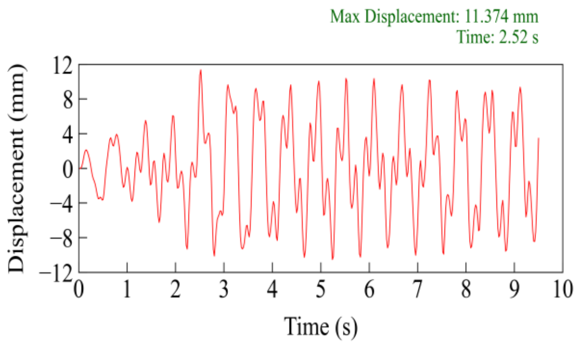

(a)

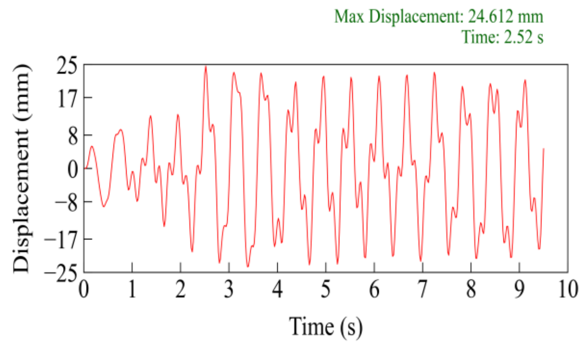

(b)

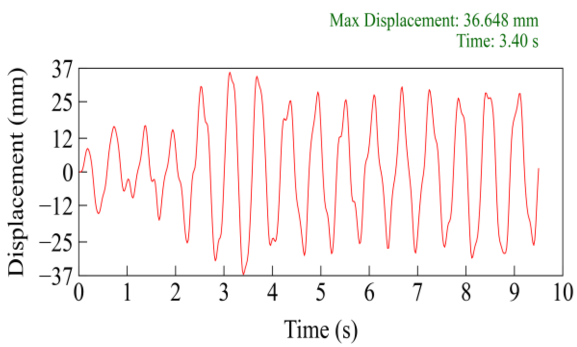

(c)

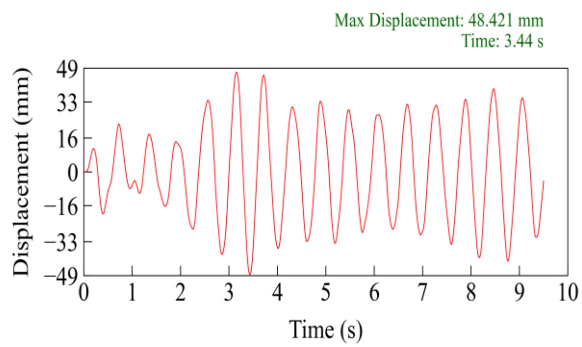

(d)

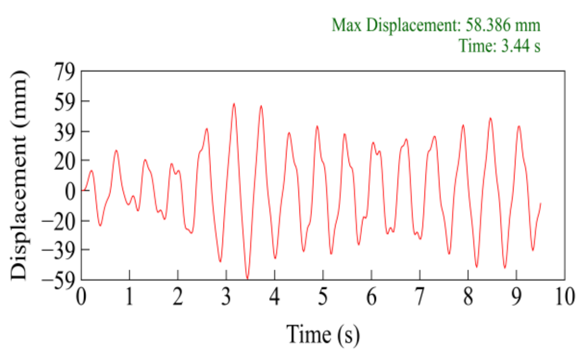

(e)

Figure 3.8: Story displacement of Model – 1: (a) 1st story, (b) 2nd story, (c) 3rd story, (d) 4th story, and (e) 5th story

3.8.2 Dynamic Displacement Response of Model - 2

Figure 3.9 shows the displacement–time response of each story in Model 2, which has the same mass applied to all floors. The displacement increases with height, and the fifth story reaches the highest value of 41.757 mm at 3.24 seconds. The fourth story behaves similarly, while the first to third stories reach their maximum displacements later, around 8.86 seconds, with smaller values between 23.278 mm and 31.836 mm. This time difference suggests that the ground motion reaches the upper stories more quickly, while the lower stories take longer to respond. This could be due to the way the mass is evenly spread, which may slow down the motion buildup at the lower levels. The displacement curves also change in shape along the height. The lower stories show wider and slower waves, while the upper stories have sharper and more concentrated motion. This shows that even with equal mass, each level responds differently depending on its position in the structure. Although the motion stays smooth and connected across all floors, the strength and timing of the movement vary with height, showing that uniform mass still creates different behavior between the lower and upper parts of the building.

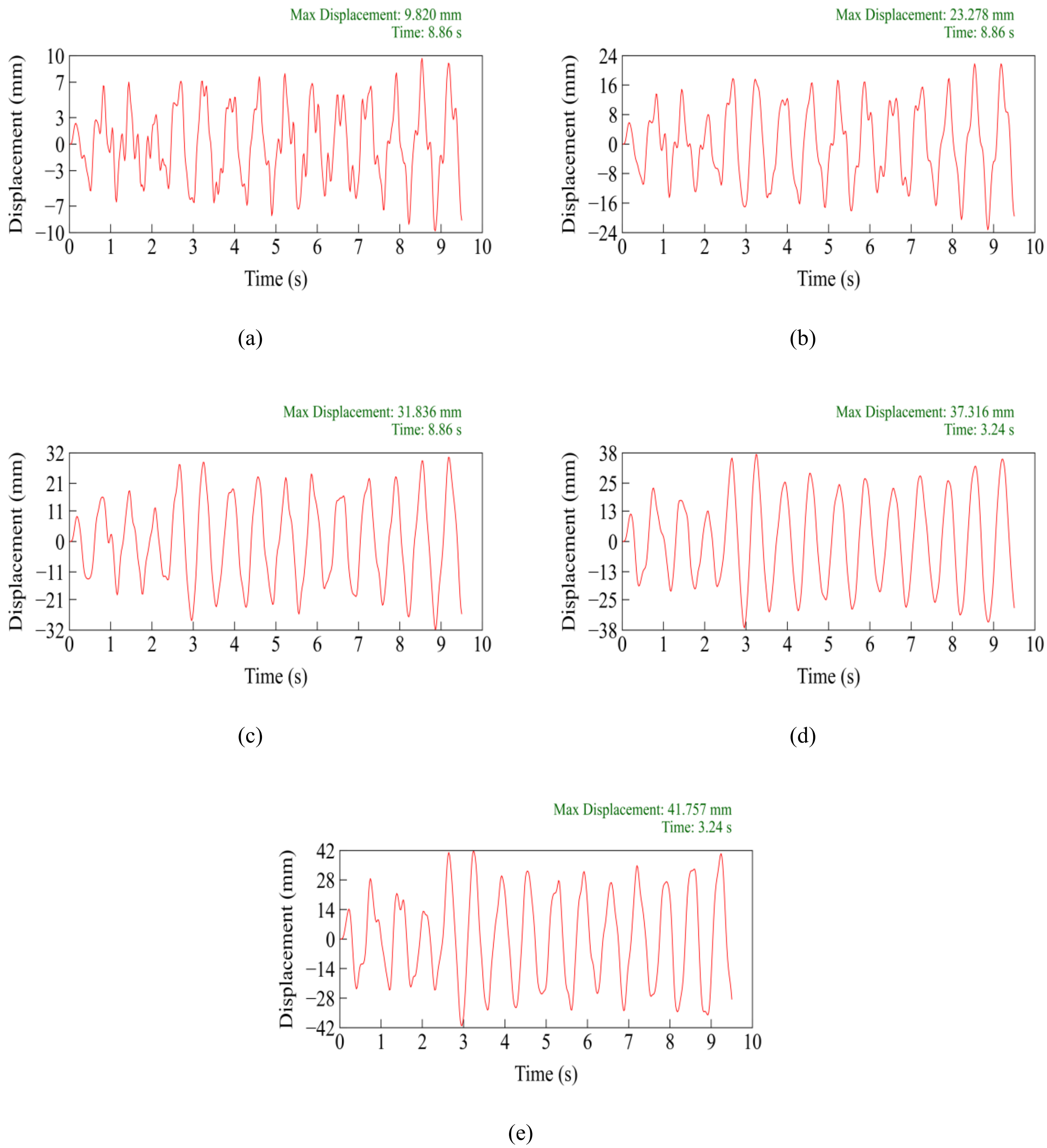

Figure 3.9: Story displacement of Model – 2: (a) 1st story, (b) 2nd story, (c) 3rd story, (d) 4th story, and (e) 5th story

3.8.3 Dynamic Displacement Response of Model - 3

Figure 3.10 presents the displacement–time response of each story in Model 3, where mass increases gradually by 25% from the first to the fifth story. The highest displacement is recorded at the fifth story with 31.237 mm at 5.70 seconds, reflecting the influence of increased mass at the top. The third and second stories show moderate peaks of 27.068 mm and 21.988 mm at later times, while the fourth story reaches its peak of 24.179 mm earlier at 1.20 seconds. The first story experiences the lowest displacement of 11.405 mm at 6.82 seconds. These results show that the motion is stronger and occurs earlier in the upper stories, likely due to the higher mass concentrated at those levels. The early response of the fourth story may indicate a local dynamic effect at mid-height, influenced by the change in mass pattern. The displacement curves at the lower stories contain denser oscillations, suggesting higher-frequency components, while the upper stories show wider curves with slower movement. This variation highlights how the 25% gradually increasing mass leads to more pronounced and earlier motion in upper levels, while lower stories respond with smaller and delayed displacements. The overall behavior confirms that changes in vertical mass distribution directly affect how and when each story responds under dynamic excitation.

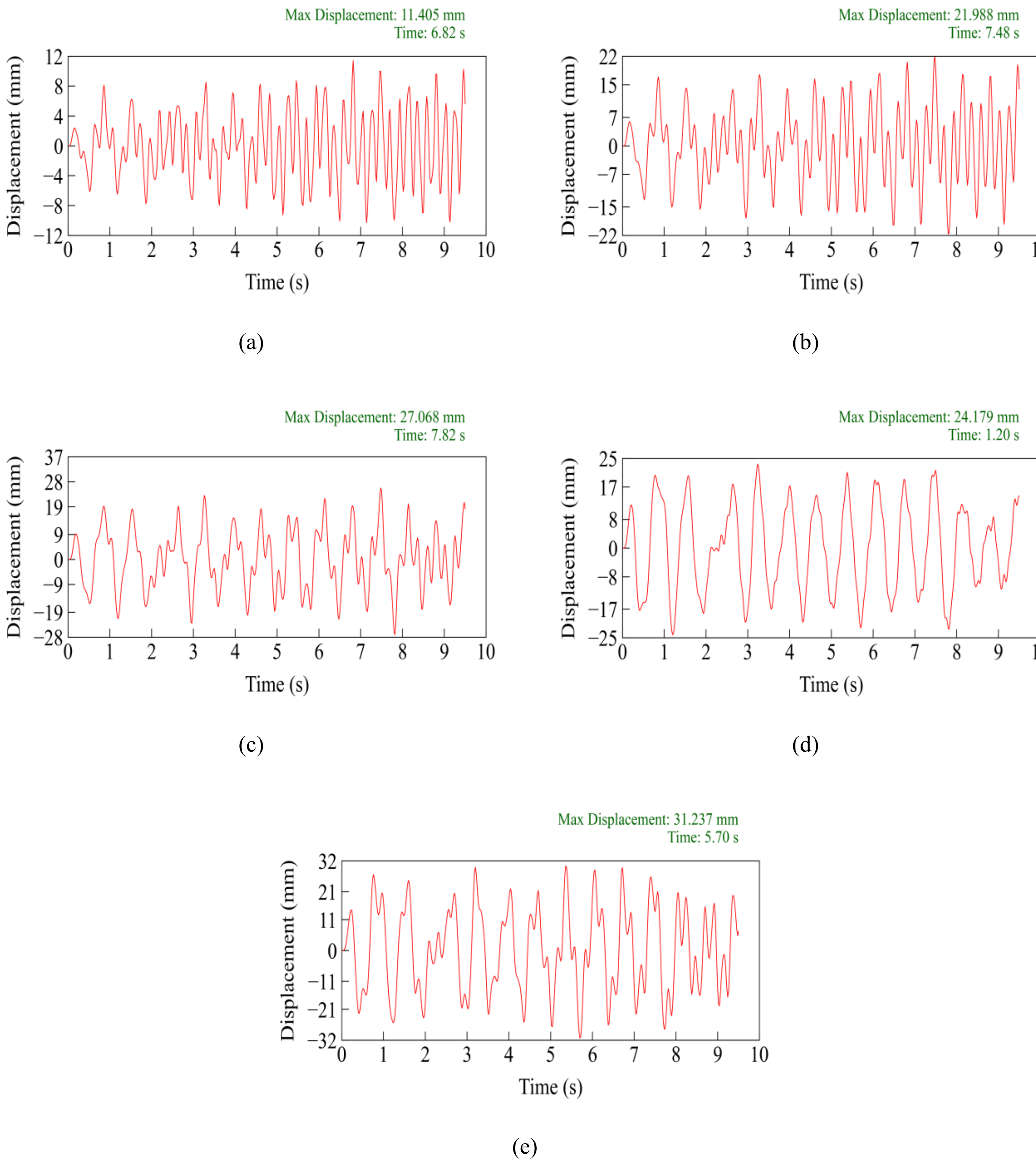

Figure 3.10: Story displacement of Model – 3: (a) 1st story, (b) 2nd story, (c) 3rd story, (d) 4th story, and (e) 5th story

3.8.4 Dynamic Displacement Response of Model - 4

Figure 3.11 illustrates the displacement–time response of each story in Model 4, where mass decreases gradually by 25% from the first to the fifth story. The maximum displacement occurs at the fifth story with 54.506 mm at 9.34 seconds, followed by the fourth story at 38.421 mm and the second story at 28.591 mm, both peaking just over 9 seconds. In contrast, the third story shows a peak of 30.162 mm at an earlier time of 2.96 seconds, and the first story reaches 15.930 mm at 8.90 seconds. This trend indicates that the motion builds more strongly in the upper stories, but the timing of response varies irregularly across the height. The earlier response of the third story may reflect a local resonance condition influenced by the changing mass profile. Compared to previous models, the displacement patterns here show that upper stories respond with higher intensity and over a longer period, while lower stories show more compact waveforms with lower amplitude. The gradually decreasing mass results in higher inertia near the base, which may limit motion in the lower stories while allowing amplified movement at the top. The waveforms remain generally smooth, but their amplitude and spacing vary significantly across the height. This highlights how a 25% decreasing mass distribution influences both the shape and timing of dynamic response, producing a more top-sensitive behavior under excitation.

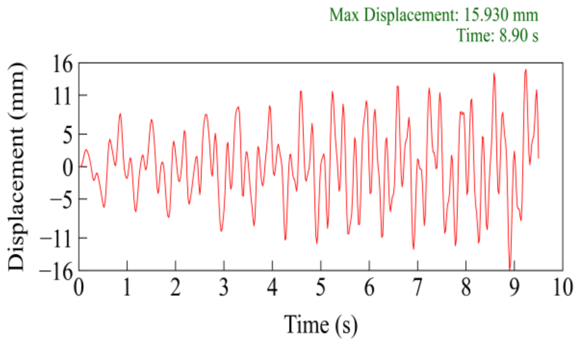

(a)

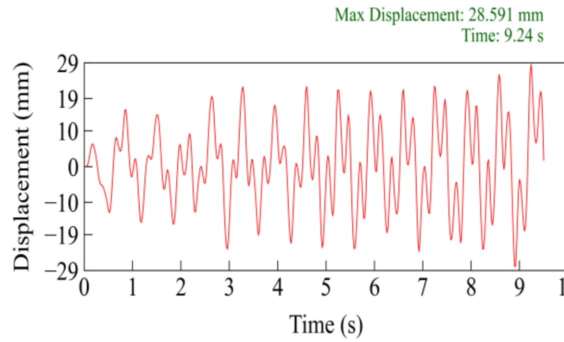

(b)

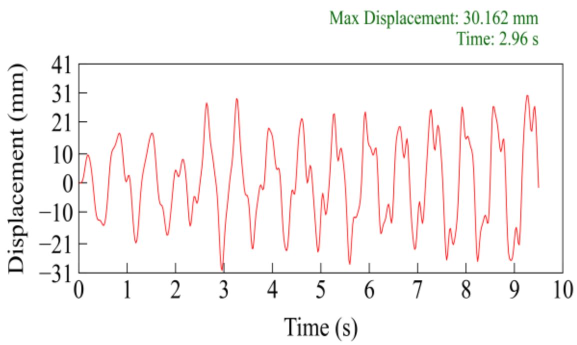

(c)

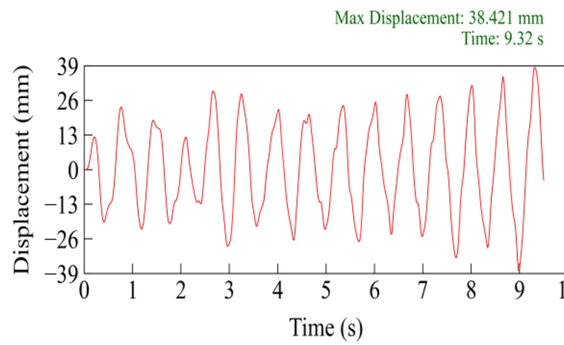

(d)

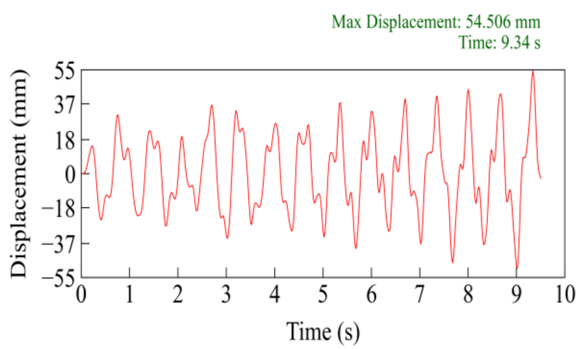

(e)

Figure 3.11: Story displacement of Model – 4: (a) 1st story, (b) 2nd story, (c) 3rd story, (d) 4th story, and (e) 5th story

3.8.5 Dynamic Displacement Response of Model - 5

Figure 3.12 shows the displacement–time response of each story in Model 5, where mass increases gradually by 50% from the first to the fifth story. The maximum displacement occurs at the fifth story with 54.723 mm at 3.00 seconds, followed closely by the fourth story at 45.994 mm, also at 3.00 seconds. The third, second, and first stories show smaller displacements of 35.850 mm, 27.686 mm, and 12.923 mm, respectively, all peaking near 2.94 seconds. The close timing of peak responses across all stories suggests a synchronized structural reaction, but the difference in displacement magnitude reflects the influence of the mass distribution. The waveform shapes shift from tighter and less regular patterns in the lower stories to broader and more defined cycles in the upper stories. Each story exhibits a noticeable damping pattern, with early peak displacement followed by a gradual reduction in amplitude over time. This indicates that the dynamic energy from the excitation is absorbed and reduced by the structure as time progresses. The greater mass near the top leads to more amplified and smoother motion at upper levels, while the lower stories respond more stiffly and decay faster. Compared to other models, this 50% gradually increasing mass distribution results in a dominant response in the upper stories, with pronounced motion occurring early and then fading steadily.

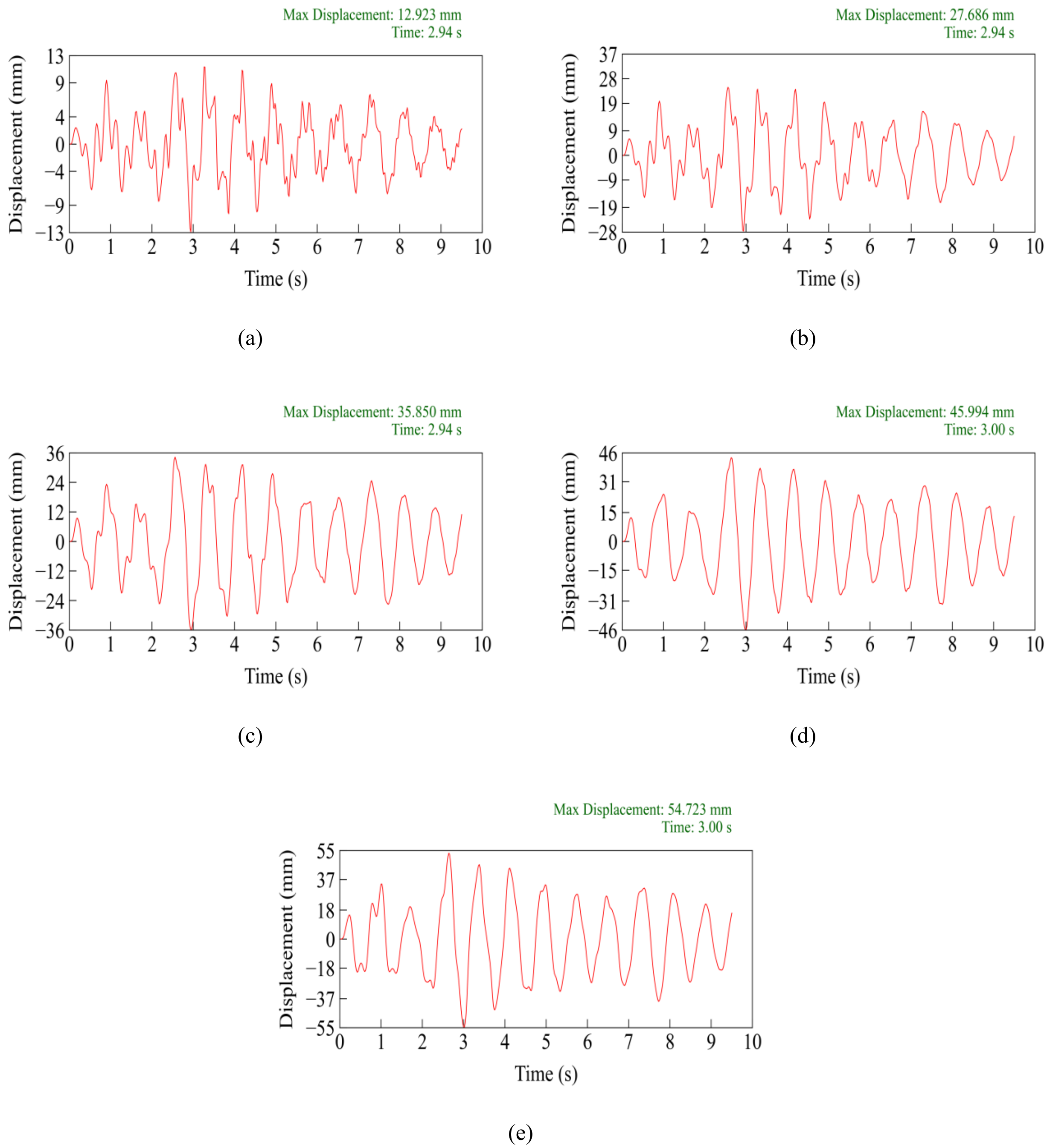

Figure 3.12: Story displacement of Model – 5: (a) 1st story, (b) 2nd story, (c) 3rd story, (d) 4th story, and (e) 5th story

3.8.6 Dynamic Displacement Response of Model - 6

Figure 3.13 illustrates the displacement–time response of each story in Model 6, where mass decreases gradually by 50% from the first to the fifth story. The fifth story shows the highest displacement of 34.483 mm, occurring very early at 0.78 seconds, indicating that the lighter top story responds quickly to the applied excitation. The fourth story reaches a peak of 27.503 mm much later, at 7.74 seconds. The first, second, and third stories exhibit lower displacements of 10.771 mm, 20.894 mm, and 23.970 mm, occurring between 3.24 and 4.30 seconds. This variation in timing and amplitude suggests that the heavier base mass delays and suppresses motion in the lower stories, while upper stories react faster due to reduced inertia. Unlike previous models, damping behavior is not significantly observed in this case. After reaching peak displacement, the oscillations maintain a relatively steady amplitude, particularly in the upper stories, indicating minimal energy dissipation over time. The displacement curves retain a consistent waveform without a noticeable decrease in amplitude, showing that the structure continues to vibrate without effective reduction in motion. This response pattern highlights that the 50% gradually decreasing mass distribution results in early and persistent motion at the top, while limiting the dynamic engagement of the lower stories.

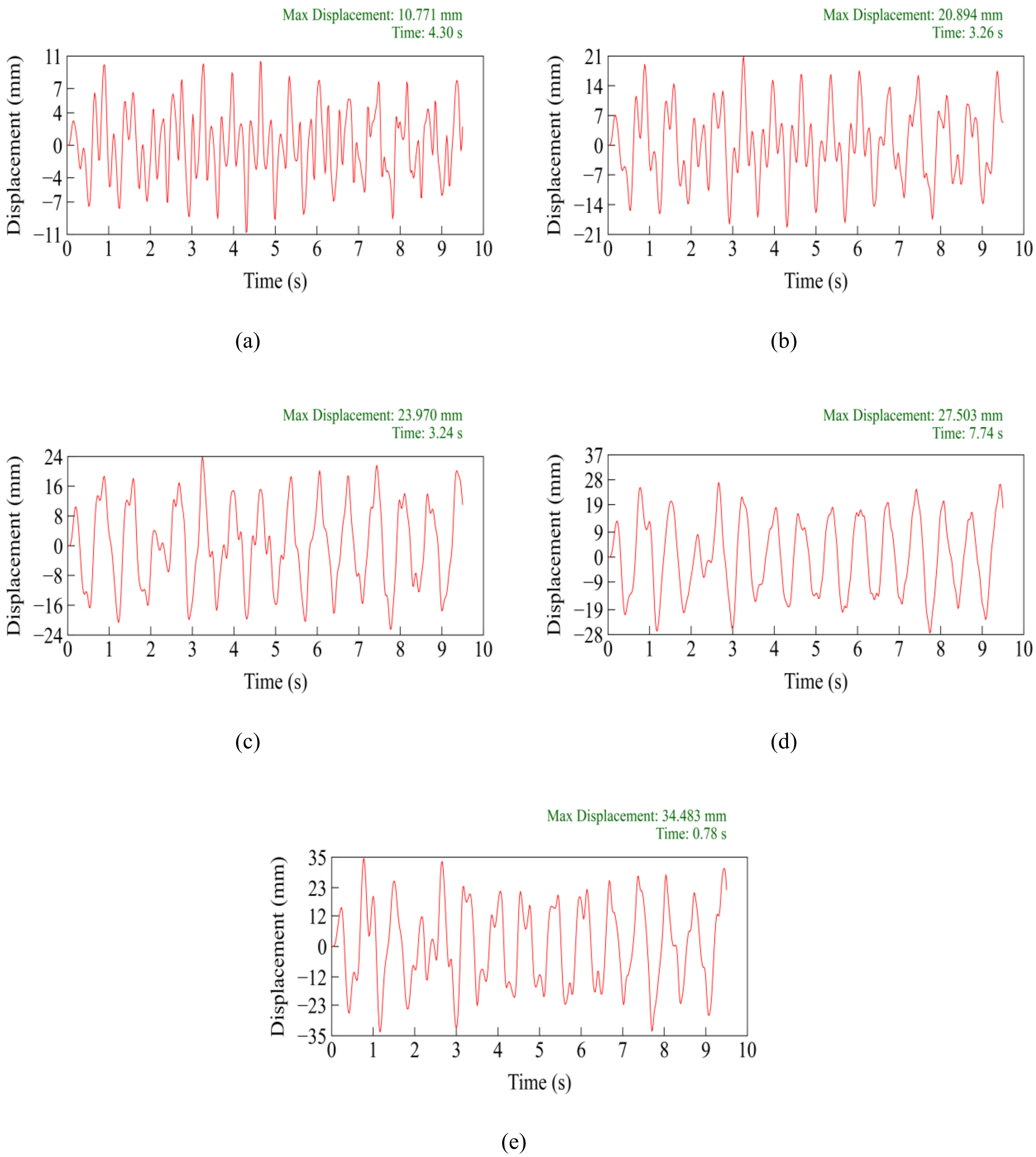

Figure 3.13: Story displacement of Model – 6: (a) 1st story, (b) 2nd story, (c) 3rd story, (d) 4th story, and (e) 5th story

3.9 Base Shear Response of Structures with Varying Mass Distributions

Figure 3.14. shows the base shear response over time for all six structural models with different mass distributions. The configuration without any added mass shows a sharp and high-frequency base shear response that stays consistent throughout the time history. Although the motion is active, there is no clear drop in amplitude, meaning that damping is not observed. A similar behavior appears in the structure with uniform mass across all stories. Its peak response is slightly delayed and broader, but the vibration continues without any clear energy reduction. When mass increases gradually by 25 percent from the bottom to the top, the waveform becomes denser and more active, yet damping is still not visible. Among all the setups, the case with 25 percent decreasing mass, where more weight is placed near the base, produces the highest base shear, reaching around 523,870 N. This arrangement increases the ground-level force and keeps the motion strong over time, with no sign of vibration fading.

In comparison, the setup with 50 percent gradually increasing mass toward the top has the second highest base shear, about 392,621 N, but shows a much different behavior. The base shear rises quickly and then slowly decreases, which clearly shows the strongest damping effect among all models. The top-heavy mass allows energy to be absorbed more effectively. The structure with 50 percent decreasing mass from top to bottom also shows some damping, but it is not as strong. The peak slowly fades, and the total base shear, at about 351,170 N, is moderate but not the lowest among the six cases. These results show how different mass layouts affect not only the strength of the base shear but also how well the structure controls vibration during dynamic loading.

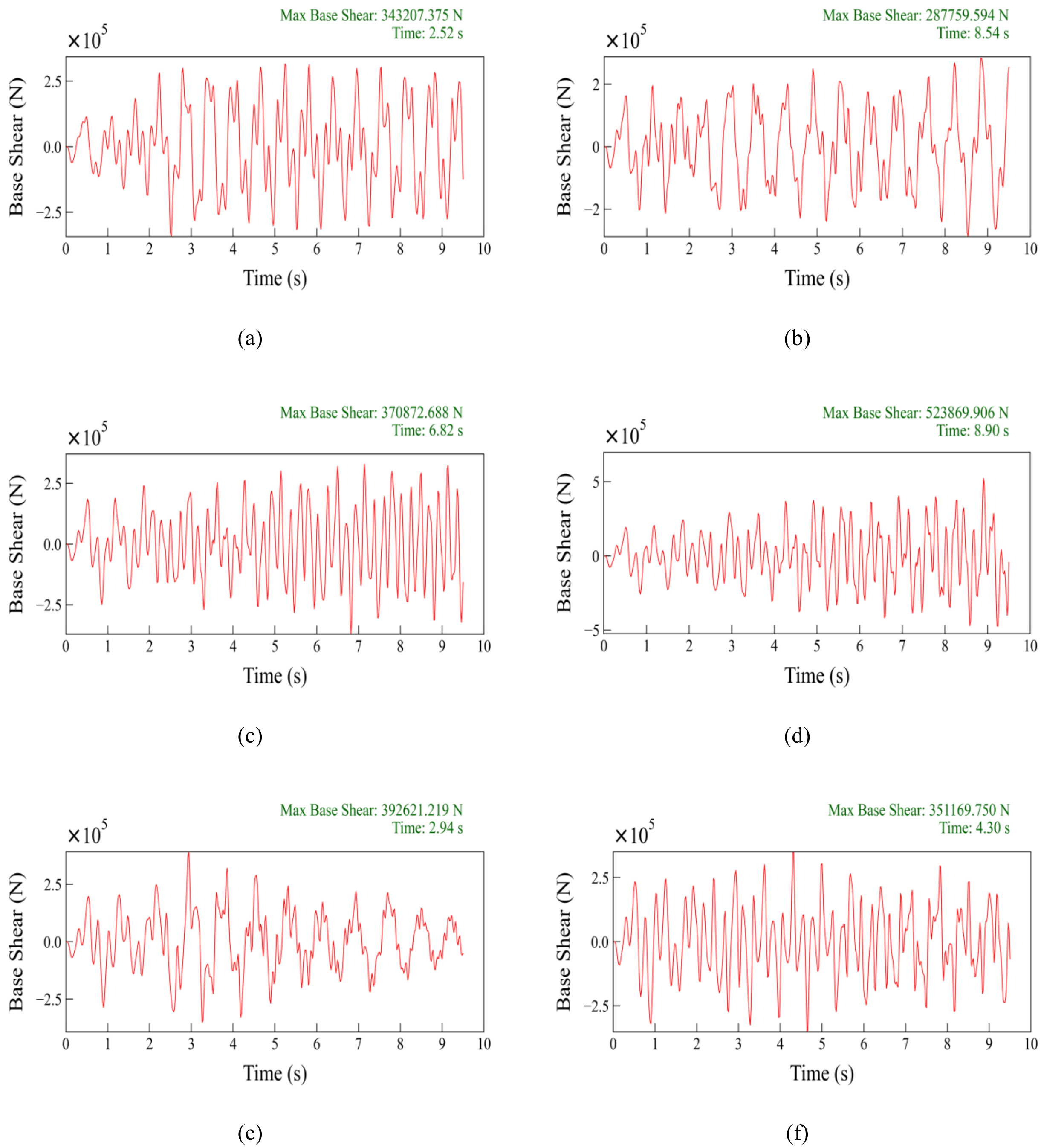

Figure 3.14: Base shear of all models: (a) 1st - Model, (b) 2nd - Model, (c) 3rd - Model, (d) 4th - Model, and (e) 5th – Model, and (f) 6th – Model

CHAPTER 4: RESULTS & ANALYSIS

4.1 Integrated Seismic Performance Evaluation

The comparative evaluation of all six structural models reveals the significant influence of vertical mass distribution on seismic dynamic response, particularly regarding natural frequencies, story displacement, and base shear. As illustrated in Figure 3.7, Model 1 characterized by uniform mass without vertical irregularity exhibits the highest natural frequency of 15.31 cycles/time, indicating greater overall stiffness and resistance to dynamic deformation. In contrast, Model 6, which features a 50 % gradually decreasing mass toward the top, demonstrates the lowest frequency at 12.18 cycles/time, reflecting increased structural flexibility and longer vibration periods. This variation in frequency response confirms that vertical mass configuration plays a crucial role in shaping the dynamic characteristics of multi degree of freedom systems.

The maximum story displacements for each model are presented in Figure 4.1. Across all configurations, displacement amplitudes increase with building height, consistent with classical dynamic amplification patterns. However, differences emerge based on how mass is distributed vertically. Model 5, which features a 50 % gradually increasing mass toward the top, records the highest fifth story displacement, approximately 54.72 mm, and maintains relatively consistent displacements across the remaining stories. This suggests a well distributed and synchronized structural response across all levels. In contrast, Models 3 and 6 show generally lower displacement values throughout, likely due to inefficient modal energy propagation caused by abrupt mass changes at the top and bottom, respectively. These outcomes highlight that both top-heavy and base heavy mass configurations can interrupt uniform dynamic engagement and reduce structural participation.

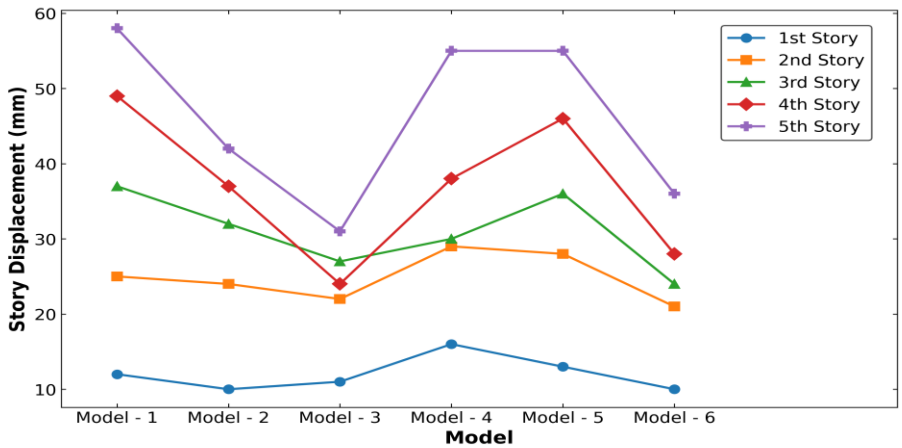

Figure 4. 1 Story displacement vs Model

Figure 4.2 illustrates the variation in base shear across the models. Model 4, which follows a 25 % gradually decreasing mass profile, produces the highest base shear, approximately 523,870 N. This elevated response is attributed to the heavier mass concentration near the base, which intensifies ground-level inertial forces. Model 2, with its uniform mass distribution, shows the lowest base shear at approximately 287,760 N. The lower base shear in this case results from evenly distributed mass that limits the buildup of concentrated inertial forces. While such a configuration reduces demand on the foundation and structural members, it may also lead to underutilization of structural capacity and weaker energy absorption during seismic loading. Model 5 demonstrates a moderate base shear of 392,621 N, indicating balanced force transmission with better overall damping behavior.

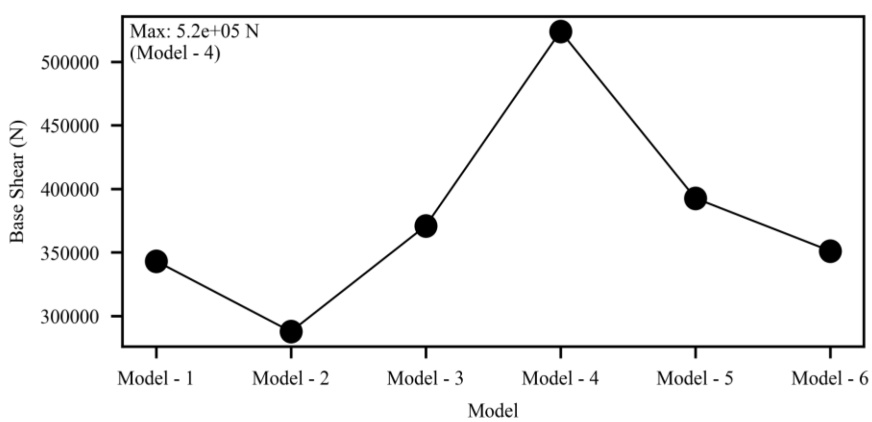

Figure 4. 2: Base shear vs Model

In terms of vertical deformation, figure 4.1 also provides insight into the story drift characteristics of each model. Model 1 displays a uniform and regular drift pattern, dominated by the first vibration mode and indicating symmetric deformation. Model 2, on the other hand, exhibits increased displacement in lower stories, suggesting that energy is absorbed near the base with reduced engagement at upper levels. Model 3 shows an irregular distribution of story drift, pointing to the presence of coupled modal effects induced by nonuniform mass. Model 4 exhibits higher displacements at the top stories, suggesting modal concentration in the upper half of the structure. Model 5 stands out by maintaining a consistent and uniform drift across all levels, supporting effective participation of all stories in dynamic response. Finally, model 6 reflects a bottom-heavy configuration, where motion is largely restricted to the upper stories and lower levels remain less engaged suggesting limited energy propagation through the structure.

4.2 Optimal Mass Distribution Strategy for Enhanced Seismic Performance

From a structural performance standpoint, both excessive and minimal displacement can compromise seismic resilience. Large displacements may cause serviceability issues and structural damage, while insufficient displacement may reflect a lack of energy dissipation capacity. Likewise, very high base shear increases the demand on foundation systems and member design, whereas very low base shear, if unaccompanied by meaningful deformation, may indicate under-engaged dynamic behavior and insufficient structural mobilization.

Considering all observations, model 5 emerges as the most favorable configuration among those studied. Its 50 % gradually increasing mass distribution produces moderate base shear, avoids excessive force demand, and achieves balanced story drift, reflecting efficient energy distribution throughout the height of the structure. Furthermore, model 5 demonstrates clear damping characteristics in its displacement time history response, where early peak displacements are followed by steady decay over time. Overall, model 5 offers the best combination of strength, deformation control, and seismic energy management, making it the most efficient and practical configuration for seismic-resistant design among the six alternatives evaluated in this study.

CHATER 5: CONCLUSIONS AND FUTURE WORKS

5.1 Conclusions

This study conducted a comprehensive numerical investigation into the effects of vertical mass distribution on the seismic response of multi-story frame structures. Utilizing linear time history analysis (LTHA) within the ABAQUS environment, six structural models with systematically varied mass configurations were assessed under the same applied occurred ground motion to evaluate their dynamic performance. The application of LTHA was essential for capturing time-dependent structural responses including natural frequencies, story displacements, drift characteristics, and base shear forces under realistic seismic loading conditions.

The analysis revealed that vertical mass irregularity significantly affects structural behavior. Models with regular or symmetric mass distributions exhibited consistent first-mode dominated responses; however, they demonstrated minimal damping, as vibrations persisted over time without significant reduction in amplitude. In contrast, irregular mass configurations introduced more complex modal behavior, energy concentration at specific stories, and non-uniform deformation patterns. These behaviors often led to either excessive displacement posing safety and serviceability risks or insufficient deformation, which compromises the structure's ability to dissipate seismic energy effectively.

Among all the evaluated models, the configuration with a 50 % gradually increasing mass toward the top (model 5) exhibited superior dynamic performance compared to the other mass distribution schemes. It produced a moderate base shear response, maintained a uniform and balanced story drift distribution, and demonstrated significant damping behavior, provided sufficient stiffness is ensured within the structural system. These results indicate that model 5 effectively balances inertial demand, energy dissipation, and deformation control qualities essential for resilient seismic performance.

This mass configuration offers practical advantages for structural design, especially in high-rise buildings and performance-based seismic engineering. Its ability to reduce excessive force demand while enhancing energy dissipation capacity supports both structural safety and economic efficiency. Furthermore, the use of LTHA in this study proved to be a powerful analytical tool, accurately capturing time-dependent seismic responses necessary for evaluating the influence of mass distribution. The results support the adoption of gradually increasing mass configurations, as exemplified by model 5, as a preferred design strategy in the development of earthquake-resistant structural systems

5.2 Limitations of the Study

While this study provides valuable insights into the seismic response of multi-story frame structures with vertical mass irregularities, several limitations should be acknowledged to ensure proper interpretation of the findings. These limitations stem from necessary simplifications in the modeling approach, constraints in computational capacity, and scope restrictions in the analysis framework. Although the adopted methodology was appropriate for the study objectives, certain aspects of real-world structural behavior could not be fully captured. The following points summarize the key limitations that may affect the generalizability and completeness of the results:

1. **One-Directional Ground Motion Input:** The seismic excitation applied in this study was restricted solely to the horizontal longitudinal direction. In real earthquake scenarios, structures are typically subjected to complex ground motions that involve multi-directional shaking, including transverse and vertical components. By excluding these components, the study may not fully capture torsional behavior or the complete dynamic response, particularly in cases where asymmetry or eccentricity exists.

2. **Exclusive Focus on Vertical Mass Irregularity:** This research considered only vertical mass irregularity where mass varies from floor to floor along the building height. However, real buildings may exhibit horizontal irregularities, such as eccentric mass placements or asymmetrical layouts, which can lead to torsional coupling and uneven lateral deformation. Not accounting for these aspects limits the generalization of the findings to structures with more complex irregularities.

3. **Simplified Single-Bay Frame Model**: The model adopted for the simulation was a single bay, single-span moment resisting frame. Although this helps to reduce computational complexity and allows for clearer interpretation of results, it does

not represent the true behavior of real-life multi-bay frame systems, which may exhibit significant load redistribution and inter-story interaction under seismic loads.

4. **Absence of 3D Seismic Input:** Due to computational limitations, the study only applied seismic excitation in a single direction. The lack of three-dimensional input motion which includes vertical and out-of-plane effects means that the results do not account for combined directional accelerations, which can significantly influence structural demand and deformation modes during strong ground shaking.

5. **Computational Resource Constraints:** The study was subject to limitations in computational resources, including hardware memory, processing power, and simulation run time. As a result, model complexity, number of modes extracted, time step resolution, and mesh refinement were balanced to ensure feasibility, potentially affecting the accuracy and detail of the results. These limitations also influenced the decision to use linear analysis instead of nonlinear simulations, and to omit more resource intensive components such as soil structure interaction and nonlinear material behavior.

5.3 Recommendations for Future Works

To further enhance the understanding of seismic behavior in multi-story frame structures with vertical mass irregularities, additional areas of investigation are proposed. Expanding the analytical scope and refining the modeling approach can lead to more realistic simulation of structural performance under earthquake loading. These forward-looking recommendations aim to strengthen the reliability, accuracy, and practical relevance of future studies by addressing critical aspects of structural dynamics that were beyond the scope of the present work. The following points outline key directions for future research:

1. **Incorporation of Multi-Directional Seismic Loading:** To enhance realism, future studies should apply three-directional ground motion inputs longitudinal, transverse, and vertical to better replicate actual earthquake conditions. This will enable analysis of torsional responses, out-of-plane movements, and combined

modal interactions, which are crucial for comprehensive seismic performance evaluation.

2. **Modeling of Complex Mass Irregularities:** It is recommended to include both vertical and horizontal mass irregularities, such as eccentric loading, irregular plan shapes, and concentrated heavy floors. These irregularities can trigger complex vibration patterns and significantly affect lateral stiffness, story drift, and resonance during seismic events.

3. **Application of Nonlinear Time History Analysis (NLTHA):** While this study utilized Linear Time History Analysis (LTHA), future work should adopt Nonlinear Time History Analysis (NLTHA) using the Dynamic, Implicit step in ABAQUS. This will allow simulation of material nonlinearities (e.g., concrete cracking, steel yielding) and geometric nonlinearity (e.g., large displacements), providing more realistic predictions under severe ground shaking.

4. **Use of Variable Damping Profiles:** In practice, damping characteristics vary along the height of a structure due to material composition, construction detailing, and occupancy use. Future models should implement variable damping ratios rather than a uniform value, to improve representation of energy dissipation behavior and enhance the reliability of dynamic response predictions.

5. **Inclusion of Soil–Structure Interaction (SSI):** Structural response is influenced not only by superstructure characteristics but also by foundation flexibility and soil conditions. Incorporating SSI models which simulate the interaction between the structure and underlying soil can significantly improve the accuracy and applicability of the findings, especially for buildings located in soft or liquefiable soils

REFERENCES

Aijaj, S. A., & Rahman, A. (2014). Seismic Response of Vertically Irregular RC Frame with Stiffness Irregularity at Ground Floor. International Journal of Civil Engineering Research, 5(4), 339–344.

Benaied, B., Hemsas, M., Benanane, A., & Hentri, M. (2023). Seismic analysis of RC building frames with vertical mass and stiffness irregularities using adaptive pushover analysis. Revista de La Construccion, 22(3), 597–612. Https://doi.org/10.7764/RDLC.22.3.597

De luca, f., & lombardi, l. (2017). Ec8 design through linear time history analysis versus response spectrum analysis-is it an enhancement for pbee?

Elkady, A. (2023). ABAQUS_steelmat_Generator: A tool for generating metal plastic and damage parameters for ABAQUS. Zenodo, Version V23, 4.

Elkady, A., & Elkady, A. (2023). ABAQUS_CDP_Generator: A tool for generating concrete damage parameters for ABAQUS. Zenodo, Version V23, 4.

Fanaie, N., & Kolbadi, M. S. (2019). Probabilistic seismic demand assessment of steel moment-resisting frames with mass irregularity in height. Scientia Iranica, 26(3A), 1156–1168. Https://doi.org/10.24200/sci.2017.4468

Gazette, B. (2021). Government of the People's Republic of Bangladesh Ministry of Housing and Public Works Bangladesh National Building Code 2020.

Ghanem, A., Lee, Y.-J., & Moon, D.-S. (2024). Seismic Vulnerability of Reinforced Concrete Frame Structures: Obtaining Plan or Vertical Mass Irregularity from Structure Use Change. Journal of Structural Engineering, 150(3). Https://doi.org/10.1061/jsendh.steng-12440

Hafezolghorani, M., Hejazi, F., Vaghei, R., Jaafar, M. S. Bin, & Karimzade, K. (2017). Simplified damage plasticity model for concrete. Structural Engineering International, 27(1), 68–78. Https://doi.org/10.2749/101686616X1081

Jain, P., & Sharma, A. (2024). Seismic performance of three dynamically similar buildings with different vertical irregularities. IOP Conference Series: Earth and Environmental Science, 1326(1). Https://doi.org/10.1088/1755-1315/1326/1/012014

Katti, G. B., & Balapgol, B. S. (2014). Seismic Analysis of Multistoried RCC Buildings Due to Mass Irregularity by Time History Analysis. 3(7), 614–617.

Khennane, A. (2013). Introduction to Finite Element Analysis Using MATLAB and Abaqus.

Kumar, A. P., & Samhitha, K. V. (2024). Influence of Mass Irregularities on the Seismic Behavior of Multi-Storied Using STAAD.Pro Connect Edition. Interantional Journal of Scientific Research in Engineering and Management, 08(12), 1–5. Https://doi.org/10.55041/ijsrem39349

Kumar, N., Parmar, J., Dalal, M., Samal, A., Patel, J., & Patil, Y. D. (2022). Effect of Vertical and Mass Irregularity on RCC Structure Subjected to Seismic Loading. 805, 799–805. Https://doi.org/10.38208/acp.v1.586

Liang, Q., Zhao, C., & Hu, J. (2020a). A New Elastoplastic Time-History Analysis Method for Frame Structures. Advances in Civil Engineering, 2020. Https://doi.org/10.1155/2020/8818187

Liang, Q., Zhao, C., & Hu, J. (2020b). A New Elastoplastic Time-History Analysis Method for Frame Structures. Advances in Civil Engineering, 2020. Https://doi.org/10.1155/2020/8818187

Lombardi, L., & De Luca, F. (2020). Derivation of fragility curves at design stage through linear time-history analysis. Engineering Structures, 219. Https://doi.org/10.1016/j.engstruct.2020.110900

Modal Analysis. (n.d.).

Pol, Mr. S., Dhanuskar, Dr. J., & Yadav, Dr. P. (2023). Linear and Nonlinear Analysis of G+15 Story Building with and without Shear Wall by using Time History Analysis Method. International Journal for Research in Applied Science and Engineering Technology, 11(8), 1220–1226. Https://doi.org/10.22214/ijraset.2023.55274

Pol, S. (2023). A Review Paper on Linear and Nonlinear Analysis of G+15 Story Building with and without Shear Wall by using Time History Analysis Method. International Journal for Research in Applied Science and Engineering Technology, 11(5), 7480–7484. Https://doi.org/10.22214/ijraset.2023.53482

Wakchaure, M. R. (2012). Study Of Plan Irregularity on High-Rise Structures (Vol. 1, Issue 8).

Wong, K. K. F. (2011). Seismic applications of nonlinear response spectra based on the theory of modal analysis. Procedia Engineering, 14, 1645–1652. Https://doi.org/10.1016/j.proeng.2011.07.207

Zabihullah, Singh, P., & Aryan, M. Z. (2020). Effect of (Vertical & horizontal) geometric irregularities on the seismic response of RC structures. International Journal on Emerging Technologies, 11(3), 965–974.

APPENDICES

Appendix A: List of Abbreviations

LTHA: Linear Time History Analysis

NLTHA: Nonlinear Time History Analysis

RCC: Reinforced Cement Concrete

SSI: Soil–Structure Interaction

CDP: Concrete Damage Plasticity

MDOF: Multi Degree of Freedom

SDOF: Single Degree of Freedom

CAE: Complete Abaqus Environment

FEA: Finite Element Analysis

FEM: Finite Element Method

Appendix B: Study of the Area